Resilient Design Coalition

# STEEL DAMPED SPECIAL MOMENT FRAMES FUNCTIONAL RECOVERY PREQUALIFICATION

Final Report Submitted to the PUC for Consideration in the 2026 NEHRP Provisions

CHARLES PANKOW FOUNDATION
Building Innovation through Research

kpff

UBC

Seismic Performance Prediction Platform
by Haselton Baker Risk Group

# RESILIENT DESIGN FOR FUNCTIONAL RECOVERY: PREQUALIFICATION REPORT FOR STEEL DAMPED SPECIAL MOMENT FRAMES

Final Report Submitted to the PUC
for Consideration in the 2026 NEHRP Provisions

Prepared By:

Resilient Design Coalition

Financially Supported by:

Taylor Dampers and the Charles Pankow Foundation

WORKING GROUP MEMBERS:

Ed Almeter, MS
Kristen Blowes, PhD, PE
Jared DeBock, PhD, PE
Curt Haselton, PhD, PE
Carlos Molina Hutt, PhD, PE
Huy Pham, PhD
David Welch, PhD
Reid Zimmerman, SE

October 6, 2025

# QUANTIFICATION OF FUNCTIONAL RECOVERY SEISMIC PERFORMANCE FACTORS FOR STEEL DAMPED SPECIAL MOMENT FRAMES

*Submitted: 10/6/2025*

## EXECUTIVE SUMMARY

A quantification of the functional recovery seismic performance factors for special steel moment frames with supplemental viscous damping (Steel Damped Special Moment Frame or DSMF) is performed in accordance with the proposed Section A.8.3.6 procedures of the 2026 National Earthquake Hazards Reduction Program (NEHRP) Provisions. The assessments documented herein covers the design of buildings with Buildings using the newly proposed DSMF design procedure, which is expected to be included in ASCE 7-28. For life-safety design, the response modification factor, R, is 8, overstrength factor, Ω, is 3.0, and the deflection amplification factor, $C_d$, is 4.5 for the DSMF system. Additionally, a 25% base shear reduction to account for supplemental damping is used for strength checks. All designs investigated herein satisfy the life-safety design provisions of the DSMF design procedure

Appendix A of the 2026 NEHRP Provisions provides additional design requirements to satisfy functional recovery performance objectives at the Functional Recovery Earthquake ($FRE_R$) level shaking. The functional recovery seismic performance factors include the functional recovery response modification coefficient, $R_{fr,}$ and functional recovery allowable story drift limit, $\Delta_{afr}$. Drift checks are performed with $C_d$ equal to 55% of $R_{fr}$, rather than 4.5, for functional recovery design. By using $C_d$ equal to 55% of R, the DSMF design procedure maintains a "$C_d$ = R" design philosophy, because the difference between $C_d$ and R is due solely to supplemental damping. The 25% base shear reduction for strength checks is taken for both life-safety and functional recovery design, according to the DSMF design procedure.

$R_{fr,}$ and $\Delta_{afr}$ were determined by developing an archetype space of different building heights, designed with various functional recovery response modification coefficients and allowable drift limits, and then selecting the combination that results in less than a 10% mean probability of Safety-Critical Structural Damage, or P[SCSD], in each performance group, and less than 20% P[SCSD] for any individual archetype, for Functional Recovery Category (FRC) A, B and C. The 10% and 20% thresholds are modified to 15% and 25%, respectively, for FRC D. All analyses are conducted at the Functional Recovery Earthquake ($FRE_R$) level shaking corresponding to a Seismic Design Category $D_{max,FRE}$ condition with two-point spectral ordinates $S_{dsfr}$ and $S_{d1fr}$ of 1.25g and 0.75g, respectively. The required values of $R_{fr,}$ and $\Delta_{afr}$ based on analysis are compared to the judgment-based limits according to Appendix A of NEHRP 2026, and the more stringent values are selected. The judgment-based limits of $R_{fr}$ are R/1.5 and R/1.25 for FRC A/B/C and FRC D, respectively. The judgment-based limits of $\Delta_{afr}$ are 1.25% and 1.75% for FRC A/B/C and FRC D, respectively.

The proposed $R_{fr}$ and $\Delta_{afr}$ and $R_{\mu fr}$ for the Steel Damped Special Moment Frame (DSMF) lateral force resisting system from the qualification assessment are presented in Table 1, in addition to $R_{\mu}$, which is a function of $R_{fr}$. The primary source of Safety-Critical Structural Damage is in the beam-column connections. However, results from the assessment show that the functional recovery performance factors are governed by the judgment-based limits. For the proposed $R_{fr}$ and $\Delta_{afr}$, lateral designs of the FRC A/B/C archetypes are largely governed by the drift limit, whereas FRC D archetypes are governed by strength requirements. Additional drift-controlled FRC D archetypes were developed to confirm that the proposed $\Delta_{afr}$ for FRC D is sufficient to meet the performance target when it is the controlling design requirement.

*Table 1 – Proposed design criteria to satisfy the Functional Recovery performance objectives for DSMF systems*

| | **FRC A/B/C** | | | **FRC D** | | |
|---|---|---|---|---|---|---|
| | **$R_{fr}$** | **$\Delta_{afr}$** | **$R_{\mu fr}$** | **$R_{fr}$** | **$\Delta_{afr}$** | **$R_{\mu fr}$** |
| Analysis results** | 6.0 | 1.25%†† | --† | 8.0 | 1.50%†† | --† |
| Judgment-based upper limit | 5.5 | 1.25% | n/a | 6.5 | 1.75% | n/a |
| **Recommendation – DSMF*** | **5.5** | **1.25%††** | **1.42** | **6.5** | **1.50%††** | **1.54** |

* Applies to DSMF systems designed according to Chapter 12 of ASCE/SEI 7. For damped systems designed according to Chapter 18 of ASCE/SEI 7, the explicit qualification procedures outlined in Section A.17 or the 2026 NEHRP Provisions should be followed.

**Analysis results include possible damage to gusset connections in the damper frame, and all analysis checks.

† $R_{\mu fr}$ is only calculated for the recommended seismic performance factors

†† When computing drifts for steel damped special moment frames, use $C_{dfr}$ of 4.4 for FRC A/B/C and 3.6 for FRC D.

# Contents

# 1. INTRODUCTION

This report documents the quantification of the functional recovery seismic performance factors for special steel moment frames with supplemental viscous damping (Steel Damped Special Moment Frame or DSMF), designed per the prescriptive design approach outlined in Chapter 12 of ASCE/SEI 7. Quantification of the functional recovery seismic performance factors is performed in accordance with the proposed Section A.8.3.6 procedures of the 2026 National Earthquake Hazards Reduction Program (NEHRP) Provisions. The functional recovery seismic performance factors include the functional recovery response modification coefficient, $R_{fr,}$, and functional recovery allowable story drift limit, $\Delta_{afr..}$

## 1.1. DSMF System Overview

The DSMF system that is the focus of this report was originally qualified as a proprietary system with the International Code Council Evaluation Service (ICC-ES) known as the Taylor Damped Moment Frame (TDMF$^{TM}$) and is currently being considered for adoption into ASCE/SEI 7 as a general prescriptive design process for a Steel Damped Special Moment Frame system (DSMF). The DSMF system combines steel special moment frames (SMFs) with supplemental damper frames (DF) that implement fluid viscous dampers. The SMFs act as the primary lateral force resisting system (LFRS) while DFs provide energy dissipation to the system, thus reducing overall seismic response.

The DSMF system can be configured in three basic types which varies the amount of interaction between the SMFs and DFs. Type I systems have no shared elements between the SMF and DF while Types II and III have fully-shared and partially-shared elements, respectively. An illustration of the different DSMF system types is shown in Figure 1. An example plan layout for a Type I system is shown in Figure 2. Dampers can be configured in Chevron, V-type (inverted chevron), Diagonal or 2-story X configurations, where the damper is in-line with the extender brace assembly within the DF (see Figure 3). Additionally, dampers can be arranged in a Modified Chevron with Horizontal Dampers (MCHD) configuration where the dampers are installed horizontally, as shown in Figure 4.

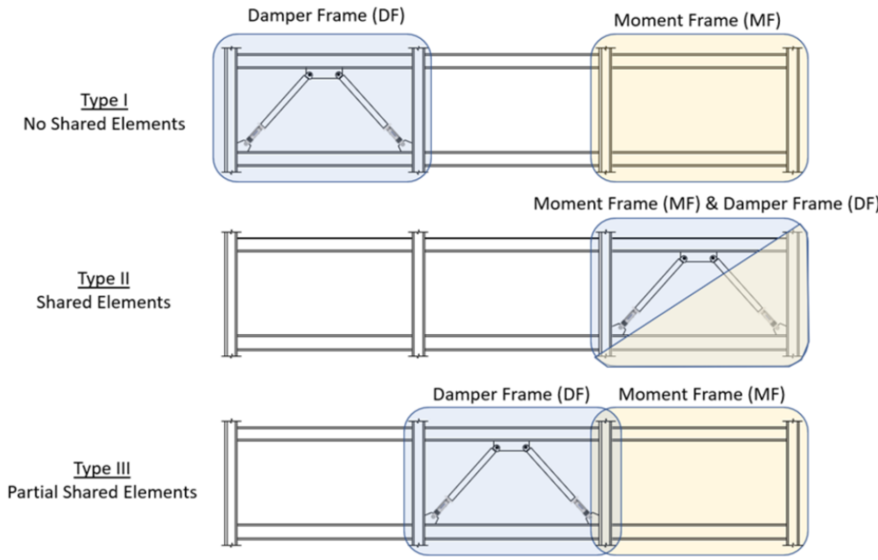


*Figure 1. Illustration of various DF and SMF configurations addressed by the TDMF™ design procedure. Elevation view. Image adapted from Figure 1 of ICC-ES (2023).*

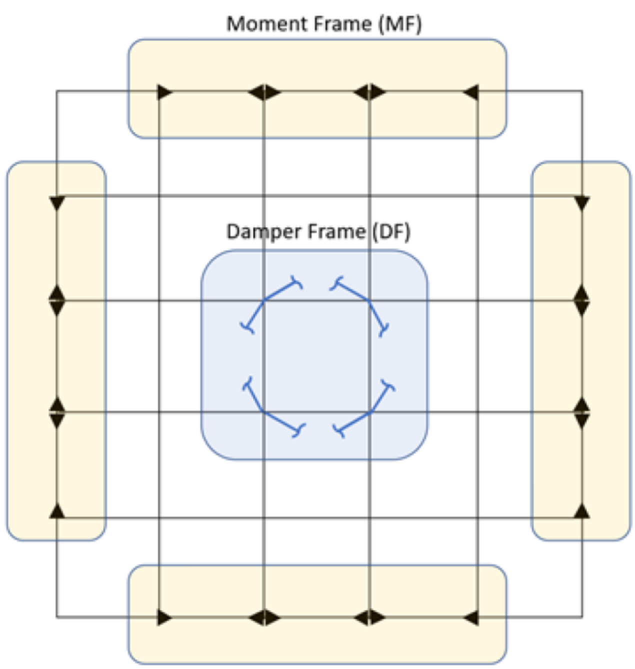


*Figure 2. Example plan view of a Type I system that has no shared elements between the MFs and DFs. Image adapted from Figure 2 of ICC-ES (2023).*

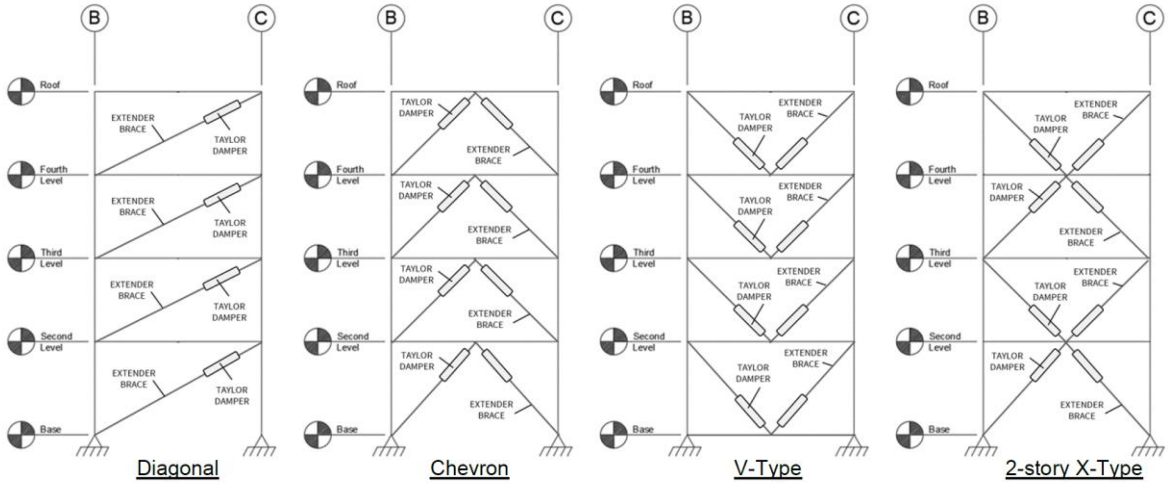


*Figure 3. Common in-line damper configurations. Image adapted from Figure 3 of ICC-ES (2023).*

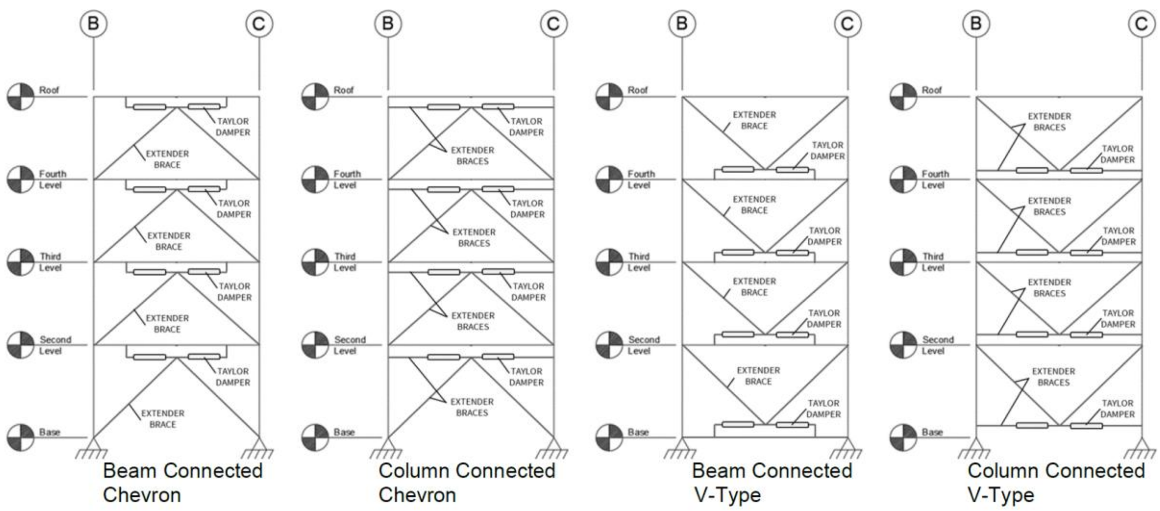


*Figure 4. Common damper configurations for modified chevron with horizontal dampers. Image adapted from Figure 4 of ICC-ES (2023).*

## 1.2. DSMF Design Procedure

The life-safety design procedure for the DSMF system is documented by ICC-ES Evaluation Service Report ESR-4679 (ICC-ES, 2023) which evaluated the system in accordance with Section 12.2.1.1 of ASCE/SEI 7 (ASCE, 2022) and ICC-ES AC494 (ICC-ES, 2018) as an alternative structural system. The evaluation process of the life safety procedure was conducted in a collaborative project between Haselton Baker Risk Group, J.R. Harris and Company, Englekirk, University of California, Los Angeles and Taylor Devices Inc. (DeBock et al. 2023; Welch and DeBock, 2023; Welch et al. 2023a,b).

The DSMF design procedure requires that the SMF lateral system is designed with an approach that follows ASCE 7 chapter 12 design requirements for Modal Response Spectrum Analysis using a 5% damped design spectrum, but with modifications that reduce the response to indirectly account for the effects of supplemental viscous damping. The modifications include:

1. A 25% reduction in the design base shear that is used for strength design of the SMF, consistent with the maximum base shear reduction allowed for damped systems according to chapter 18 ASCE 7.
2. Deflection amplification factor ($C_d$) equal to 55% of the response modification factor (R) to indirectly account for reductions in response due to 25% supplemental damping at the design intensity—an approximate 45% reduction in response.

Note that by using $C_d$ equal to 55% of R, the DSMF design procedure maintains a "$C_d$ = R" design philosophy, because the difference between $C_d$ and R is due solely to supplemental damping that is provided by the DF's. I.e. the design procedure could have required $C_d$ = R, but then allowed deflections to be reduced by 45% to account for supplemental damping, to achieve the same result.

The DF's are proportioned to provide 25% damping at the DE intensity using dampers with a velocity exponent (α) of 0.4. The reason for requiring a specific damping ratio and velocity exponent is so that the reduction in response due to damping is consistent; therefore, the 25% base shear reduction for strength design and $C_d$ equal to 55% of R are always applicable, eliminating the need for design iterations to account for damping effects. As a result, the design of the DF and the SMF are decoupled in the DSMF design procedure, except for shared members between them (e.g. shared columns in Type II and Type III DSMF systems).

### 1.3. Assessment of DSMF for Functional Recovery Design

Recommended functional recovery seismic performance factors for DSMF buildings are determined by analyzing a suite of archetype DSMF buildings with different heights, designed with various functional recovery response modification coefficients and allowable drift limits. Design of the archetypes was performed using the automated design capability of SP3 (www.sp3risk.com) and engineering demand parameters (e.g., story drift ratios, peak floor accelerations, etc.) were estimated using SP3's Response Prediction Engine, which while calibrated based on extensive nonlinear response history analyses, does not perform nonlinear response history analyses of the specific archetype directly.

Performance assessments of each modeled archetype building are conducted following FEMA P-58 (FEMA, 2018a) and ATC-138 recommendations to quantify the probability of safety-critical structural damage (P[SCSD]) for each archetype (Blowes et al., in review). In accordance with the proposed Section A.8.3.6 procedures of the 2026 NEHRP Provisions, only structural components are included in the performance models for this assessment. The triggering of SCSD is governed by the assigned safety class for a given component and damage state according to the ATC-138 methodology. The safety class controls what percentage of components, in each story and direction, that can be in each damage state or greater, prior to triggering SCSD in the building. The P[SCSD] serves as an acceptable proxy for the probability of exceeding the target functional recovery times for structural-only models, as outlined in section CA.8.3.6 of the 2026 NEHRP Seismic Provisions.

The functional recovery seismic performance factors are selected such that archetypes designed for that $R_{fr}$ and $\Delta_{afr}$ result in less than a 10% mean P[SCSD] in each performance group and less than 20% P[SCSD] for any individual archetype for Functional Recovery Category (FRC) A, B and C. The 10% and 20% are modified to 15% and 25%, respectively, for FRC D. These limits are in accordance with the proposed Section A.8.3.6 procedures of the 2026 National Earthquake Hazards Reduction Program (NEHRP) Provisions and are subjected to upper bounds therein. All analyses are conducted at the Functional Recovery Earthquake ($FRE_R$) level shaking corresponding to a Seismic Design Category $D_{max,FRE}$ condition with two-point spectral ordinates $S_{dsfr}$ and $S_{d1fr}$ of 1.25g and 0.75g, respectively.

## 2. ANALYSIS METHODS

The methods used to perform the functional recovery prequalification analyses are presented in this section. Discussion of performing design iterations and acceptance criteria for the DSMF system are discussed in Section 2.1. Background information on the fragility functions used to estimate SCSD is provided in Section 2.2. The details of the archetype design space used for analysis are provided in Section 2.3. The estimation of structural responses, or engineering demand parameters (EDPs), is discussed in Section 2.4.

### 2.1. Design Iteration and Acceptance Criteria for Seismic Performance Factors

For each individual archetype, design iterations are carried out using values of $R_{fr}$ and $\Delta_{afr}$ across the ranges of 1 through R (i.e., up to the response modification coefficient used in life-safety design) and 0.5% through 2.0% (i.e., up to the maximum allowable story drift ratio for Risk Category II structures), respectively. The Response Modification Factor, R, is 8 for DSMF systems, in accordance with *ICC-ES ESR 4769* (ICC-ES, 2023). These design iterations are performed using the SP3 design engine that estimates strength and stiffness of each design to estimate appropriate structural responses and subsequent estimates of SCSD.

In each performance group, the combination of $R_{fr}$ and $\Delta_{afr}$ is deemed to be acceptable if the mean P[SCSD] is less than 10%, and the maximum P[SCSD] across all archetypes in the performance group is less than 20% for quantifying the functional recovery seismic performance factors for Functional Recovery Category (FRC) A, B and C. For FRC D, the mean and maximum P[SCSD] across all archetypes in a performance group must be less than 15% and 25%, respectively. The recommended design values for a particular system are taken as the most restrictive across all performance groups, rounded to the nearest increment considered (0.5 for $R_{fr}$ and 0.25% for $\Delta_{afr}$).

The requirements of the proposed Section A.8.3.6 procedures of the 2026 NEHRP Provisions impose that Rfr and Δafr shall not be taken less than R/1.5 and 1.25% for FRC A, B and C and R/1.25 and 1.75% for FRC D. These "judgment-based" upper limits on seismic performance factors correspond to values required for Risk Category IV (FRC A, B, and C) and Risk Category III (FRC D) structures when performing life safety design. Additionally, to verify the strength and stiffness coupling inherent to each design variant, each archetype model is re-assessed under an independent strength and stiffness assumption, i.e., where additional strength prescribed by $R_{fr}$ does not add additional stiffness to the building. Analysis outcomes from the independent-strength-and-stiffness assessment are checked to ensure the maximum P[SCSD] does not exceed the acceptance criteria (20% for FRC A/B/C and 25% for FRC D), where applicable. The judgment-based upper limit and the independent-strength-and-stiffness check provide a reasonable limit, preventing too great of a reliance on the analytical results and recognizing the historical precedent set by the higher Risk Categories.

### *2.1.1. Safety-Critical Structural Damage (SCSD)*

The triggering of SCSD is governed by the assigned safety class for a given component and damage state according to the ATC-138 methodology (ATC, 2021). The safety class controls the percent of components, in each story and direction, that can be in each damage state or greater, prior to triggering SCSD. A summary of the ATC-138 safety class descriptions and acceptance thresholds is shown in Table 2. The components considered for SCSD for DSMF are described in Section 2.2.

*Table 2. ATC-138 safety-class definitions for triggering SCSD (ATC, 2021).*

| Safety Class | Description | Acceptance Threshold[a] |
|---|---|---|
| 0 | Slight damage that is not a safety concern and will never trigger an unsafe placard | N/A |
| 1 | Moderate damage that may be visually concerning, but does not substantially reduce the lateral strength of the component. | 50% |
| 2 | Severe damage that causes substantial loss of lateral strength of the component, but does not substantially reduce its vertical load carrying capacity. | 25% |
| 3 | Severe damage that compromises both lateral and vertical load carrying capacity of the component. | 10% |

[a] Percentages reflect the upper quantity of components, in each story and direction, that can be in a safety class of interest before triggering safety-critical structural damage (SCSD)

## 2.2. Fragility Functions for the Steel Damped Special Moment Frame (DSMF) System

Fragility functions are used to relate structural responses to likely damage and consequences. Fragility functions are commonly modeled by a lognormal distribution defined by a lognormal mean (θ) and standard deviation (β). For a given structural component, sequential damage states (DSs) can be represented by individual fragility functions that represent the likelihood of a distinct level of damage and corresponding level of repair effort and consequences. Additionally, damage states may be mutually exclusive, where a single fragility function may be used to represent multiple outcomes (i.e., sub-damage states) where the likelihood of each is given a weighting that sums to unity (e.g., 0.25 + 0.75 = 1). The fragility functions used in the current study will use both sequential and mutually exclusive damage state definitions. More general background information on fragility functions and damage state development can be found in FEMA P-58-1 (FEMA, 2018a).

The following sub-sections provide details on the structural component fragility functions, including:

- Fluid viscous damper assemblies;
- Steel special moment frame beam-to-column connections;
- Bolted shear tab gravity connections;
- Column base plates;
- Welded column splices.

Foundation elements are considered rugged in the current analysis. Fragility functions for foundation elements were not developed during the FEMA P-58 project and foundations elements are specifically included in the list of acceptable rugged components in Appendix I of FEMA P-58-1 (FEMA, 2018a). Further, the estimation of structural responses assumes a fixed base condition at grade, without any consideration of foundation flexibility or soil structure interaction. Additionally, column base plates and column splices are only populated within the moment frames that comprised the lateral force resisting system (LFRS).

### *2.2.1. Fluid Viscous Damper Fragilities*

Viscous damper (VD) fragilities were developed within a previous study conducted for Taylor Devices (Welch et al. 2023c). The fragility development is based on direct discussion with Taylor Devices on possible limit states of viscous dampers (Taylor Devices, 2023).

The stringent design and testing requirements of VDs, as outlined by Sections 11 and 12 of ICC-ES ESR-4769 (ICC-ES, 2023) ensures proper behavior of a VD within the desired stroke capacity. The testing and design requirements are based on those outlined by ASCE 7-22 Section 18.2.4. A key aspect of the TDMF design procedure, critical for fragility development discussion, is that the qualification studies conducted using the FEMA P695 (FEMA, 2009) framework used the exceedance of damper stroke as a conservative definition of global collapse. This indirectly incorporates an additional margin of safety into the method, where the probability of reaching specified damper strokes (and thus damper damage), rather than collapse, meets FEMA P695 acceptance criteria at the $MCE_R$ intensity. Additionally, the TDMF™ design procedure requires that damper strokes be required to accommodate 3% story drift ratio and first story strokes must be able to accommodate at least 85% of the equivalent story drift ratio at stroke exceedance in the story above (ICC-ES, 2023).

Fragility development (described in more detail in Welch et al. 2023c) used damper stroke converted to an equivalent story drift ratio as an EDP. This requires that median fragilities be defined generically in terms of multiples of the specified damper stroke, then converted to story drift ratio based on the specified stroke and damper configuration (i.e., inclination angle). The fragility functions for VD assemblies are comprised of two sequential damage states (DS).

DS1 has a median value at the specified damper stroke and is split into two mutually exclusive damage states (i.e., DS1a and DS1b). DS1a corresponds to a no damage condition and is attributed a 30% probability given that DS1 occurs. DS1b represent the failure of damper seals requiring damper replacement and it attributed a 70% probability given that DS1 occurs and is assigned Safety Class 2. DS1 is attributed a small dispersion value of 0.05 that reflects the highly engineered nature of viscous dampers and the ability to reliably achieve a specified stroke. Feedback from peer review suggested that the Safety Class for DS1b could be relaxed from 2 to 1, yet the original Safety Class of 2 in conservatively maintained for the current analysis although the suggestion is well within reason considering the nature of DS1b.

DS2 represents severe damage to the damper components with the possibility of gusset, clevis and extender brace damage. The median of DS2 is represented by stroke demands 20% above the specified stroke capacity (i.e. 1.2 times the stroke). DS2 is assigned to Safety Class 2. DS2 is attributed a dispersion of 0.1 that reflects larger uncertainty than DS1 while maintaining a logical lower tail with respect to the specified stroke capacity.

A summary of the VD fragility functions, and corresponding safety classes, is provided in Table 3. To give a sense of the drift magnitude associated with each damage state, for illustration only, Figure 5 plots fragilities corresponding to the average stroke of all $R_{fr}$ = 8 and $\Delta_{afr}$ =2% (e.g., Risk Category II parameters at the $FRE_R$) archetypes at the first story (see Section 2.3 for archetype details). Similarly, fragilities corresponding to the minimum 3% drift accommodation requirement are provided in Figure 6. The VD fragilities corresponding to a 2% drift limit in Figure 5 represent an upper bound, while the VD fragilities at the minimum 3% drift accommodation requirement (Figure 6) represent the lower bound of damper capacity, regardless of the design drift limit for the moment frame. A key clarification is that the required stroke capacity at the design level ($d_{ji,s}$) is scaled by an overstroke factor ($\Omega_d$) to obtain the final specified stroke. The overstroke factor varies based on the number of stories in the building, with shorter buildings receiving a higher overstroke factor compared to taller buildings. An example of design stroke calculations is provided in Figure 7 for an 8-story archetype designed to $R_{fr}$ = 8 and $\Delta_{afr}$ =2% at the $FRE_R$. The figure shows that the design drift profile from MRSA analysis gives strokes corresponding to approximately 1.2% drift. The overstroke factor ($\Omega_d$) has a value of 3.0 according to the TDMF design procedure for 8-story buildings. This results in specified strokes of 5 inches (rounded to nearest inch) in the bottom stories that correspond to story drift ratios of approximately 4%. These stroke capacities are specified following the design procedure and meet the 3% minimum drift accommodation requirement. For completeness, if the same archetype was designed for a 1% drift limit (i.e., $\Delta_{afr}$ =1%), the two lowest stories would have damper strokes governed by the 3% drift accommodation requirement. More details on the TDMF design procedure can be found in ICC-ES ESR-4769 (ICC-ES, 2024).

*Table 3. Viscous damper assembly fragility damage states and corresponding safety classes.*

| Damage State[a] | Median (θ)[b] | β | Safety Class[c] | Damage Description | Repair Measures |
|---|---|---|---|---|---|
| DS1a (0.3) | 1.0 | 0.05 | 0 | No damage. | No repair required. |
| DS1b (0.7) | 1.0 | 0.05 | 2 | Leaking of seal. | Full replacement of damper. |
| DS2 | 1.2 | 0.35 | 2 | Damper severely damaged. Gusset and brace damage possible. | Full replacement of damper. Gusset and brace modifications required for repair. |

[a] Mutually exclusive damage states (e.g., DSXa and DSXb) include the probability of occurrence in parentheses
[b] Fragility function is a lognormal distribution with median and standard deviation of θ and β, respectively. The tabulated EDP is fraction of damper stroke that is converted to an equivalent story drift ratio based on configuration.
[b] SC 1 = 50%, SC 2 = 25%, SC 3 = 10% allowable quantity of damaged components per direction per story; SC 0 cannot cause SCSD

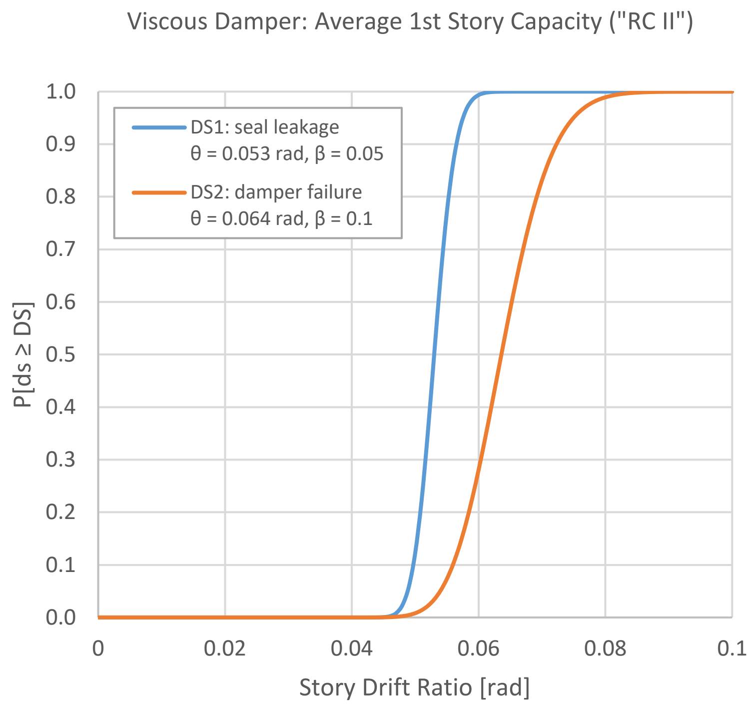


*Figure 5 – Fragility functions for viscous damper assemblies: medians are based on the average 1st story stroke of all archetypes with $R_{fr}$ = 8 and $\Delta_{afr}$ = 2%.. Damage state details are provided in Table 3.*

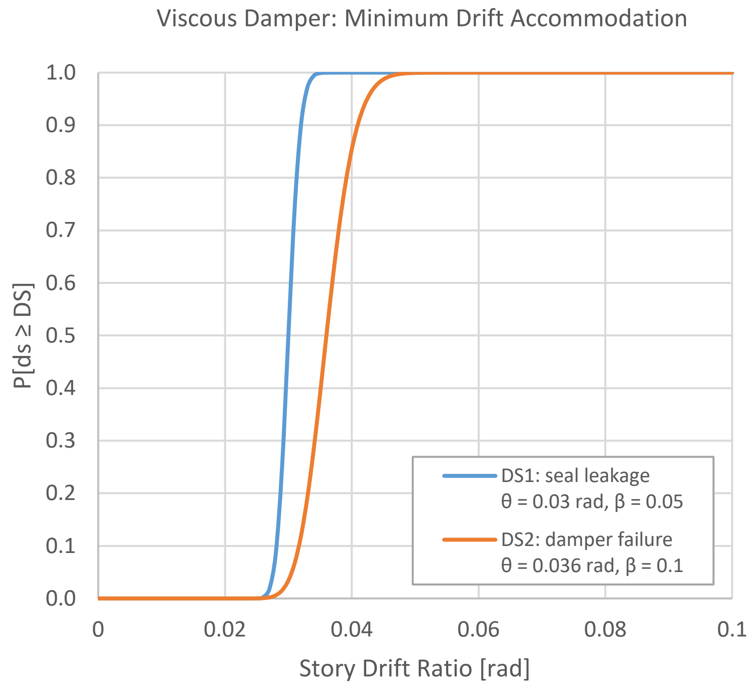


*Figure 6 – Fragility functions for viscous damper assemblies: medians are based on 3% drift ratio accommodation. Damage state details are provided in Table 3.*

| *Damper Stroke Calculations: N = 8, $R_{fr}$ = 8, $\Delta_{afr}$ = 2%, $L_{bay}$ = 30ft, Chevron Configuration* | | | | | | | | | | |
|---|---|---|---|---|---|---|---|---|---|---|
| Story | Story Height [ft] | Bay Width [ft] | MRSA Drift Ratio | MRSA Drift [in] | Damper Angle [deg] | Design Stroke $d_{ji,s}$ [in] | Overstroke Factor $\Omega_d$ | Overstroke $d_{ji,s}*\Omega_d$ [in] | Specified Stroke (rounded) [in] | Drift Ratio at Overstroke $SDR_{\Omega d}$ |
| 8 | 13 | 30 | 1.0% | 1.60 | 40.9 | 1.21 | 3 | 3.64 | 4 | 3.4% |
| 7 | 13 | 30 | 1.1% | 1.70 | 40.9 | 1.29 | 3 | 3.86 | 4 | 3.4% |
| 6 | 13 | 30 | 1.1% | 1.75 | 40.9 | 1.32 | 3 | 3.96 | 4 | 3.4% |
| 5 | 13 | 30 | 1.1% | 1.75 | 40.9 | 1.32 | 3 | 3.96 | 4 | 3.4% |
| 4 | 13 | 30 | 1.1% | 1.75 | 40.9 | 1.32 | 3 | 3.96 | 4 | 3.4% |
| 3 | 13 | 30 | 1.1% | 1.76 | 40.9 | 1.33 | 3 | 4.00 | 4 | 3.4% |
| 2 | 13 | 30 | 1.2% | 1.84 | 40.9 | 1.39 | 3 | 4.18 | 5 | 4.2% |
| 1 | 15 | 30 | 1.2% | 2.17 | 45.0 | 1.54 | 3 | 4.61 | 5 | 3.9% |

Drift profile at design level

$$\Omega_d = 4 - \begin{matrix} 3.5 & for\ N \le 4 \\ (N/8) & for\ 5 \le N \le 12 \\ 2.5 & for\ N > 12 \end{matrix}$$

Drift profile at final damper strokes (used to define fragility medians)

*Figure 7 – Example calculations of damper strokes and corresponding story drifts for an 8-story archetype*

### *2.2.2. Gusset Fragilities in the Damper Frame*

In the development of the damper fragilities, the connection to the frame around the damper was assumed to be rugged. In the case of pinned connections in the damper frame, the design requirements includes a criterion that the frame be able to drift to 5% interstory drift. In the case of moment-connected frames around the dampers, the requirement is that the steel sections have some ductility and capacity design, but do not need to meet the full requirements of special detailing. For this case of moment-connected frames around the dampers, other studies have shown that damage can occur to the gusset connection and that such gusset connections have shown drift capacities of ~3%, with that damage state having mutually exclusive consequences functions with a 25% change of Safety Class 2 being triggered (in the updated report version of ATC, 2021). This damage state has been included in this functional recovery performance assessment process.

### *2.2.3. Steel Special Moment Frame Beam-Column Connection Fragilities*

Steel beam-to-column moment connections are modeled with the same component fragilities that are used to model steel SMF systems that do not have supplemental damping. These are based on fragility development by Deierlein and Victorsson (2008) during the FEMA P-58 Project and are available within the FEMA P-58 fragility database. The fragilities are based on 36 sub-assembly tests, largely conducted as part of the SAC Joint Venture Project (Hamburger et al. 1999). Testing included reduced beam section (RBS) and non-RBS connections. A summary of the experimental testing considered is provided in Table 4.

*Table 4. Experimental testing used for special steel moment connection fragilities (Deierlein and Victorsson, 2008).*

| **Reference** | **Type** | $N_{test}$ |
|---|---|---|
| Ricles et al. (2004) | RBS | 5 |
| Engelhardt and Venti (2000) | RBS | 3 |
| Ricles et al. (2000) | non-RBS | 11 |
| Venti and Engelhardt (2000) | non-RBS | 1 |
| Gilton et al. (2000) | non-RBS | 1 |
| Choi et al. (2000) | non-RBS | 5 |
| Kim et al. (2000) | non-RBS | 10 |

Fragility functions for steel moment frame beam-column connections are comprised of three sequential damage states. DS1 represents the onset of local flange and web buckling and is assigned Safety Class 0. DS2 represents similar DS1 buckling but with lateral-torsional buckling in the plastic hinge region of the beam. DS2 is assigned to Safety Class 1. DS3 represents the low cycle fatigue fracture of flanges and significant strength loss. DS3 is assigned to Safety Class 2 for steel moment connections. The FEMA P-58 fragilities for steel moment connections do not distinguish between the type of connection (e.g., RBS versus non-RBS) in terms of damage state hierarchy and fragility parameters. A summary of the fragility functions is provided in Table 5. An illustration of the three damage states for special steel moment connections is provided in Figure 8. A plot of the fragility functions is provided in Figure 9.

*Table 5. Steel moment connection fragility damage states and corresponding safety classes.*

| Damage State | Median (θ)[a] | β | Safety Class[b] | Damage Description | Repair Measures |
|---|---|---|---|---|---|
| DS1 | 3.0% | 0.3 | 0 | Local beam flange and web buckling. | The likely repair state is heat straightening of the buckled flanges and web. Repair and replace partitions at connection. |
| DS2 | 4.0% | 0.3 | 1 | DS1 plus lateral-torsional distortion of beam in hinge region. | Repair will necessitate removal and replacement of distorted and or fractured portion of beam. Repair and replace partitions at connection. |
| DS3 | 5.0% | 0.3 | 2 | Low-cycle fatigue fracture in buckled region of beam. | Repair will necessitate removal and replacement of distorted and/or fractured portion of beam. Repair and replace partitions at connection. |

[a] Fragility function is a lognormal distribution with median and standard deviation of θ and β, respectively. The EDP is story drift ratio.
[b] SC 1 = 50%, SC 2 = 25%, SC 3 = 10% allowable quantity of damaged components per direction per story; SC 0 cannot cause SCSD

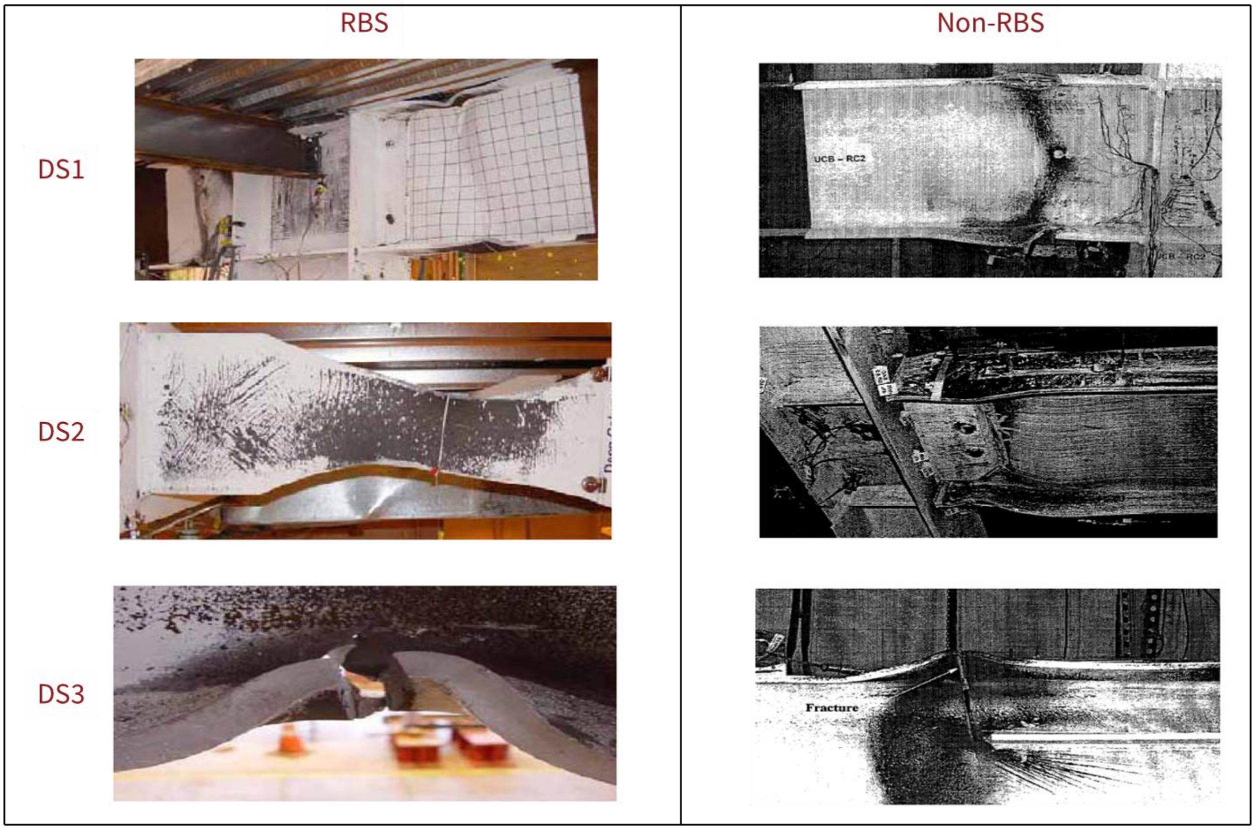


*Figure 8 – Illustration of damage states for steel special moment connections (Deierlein and Victorsson, 2008).*

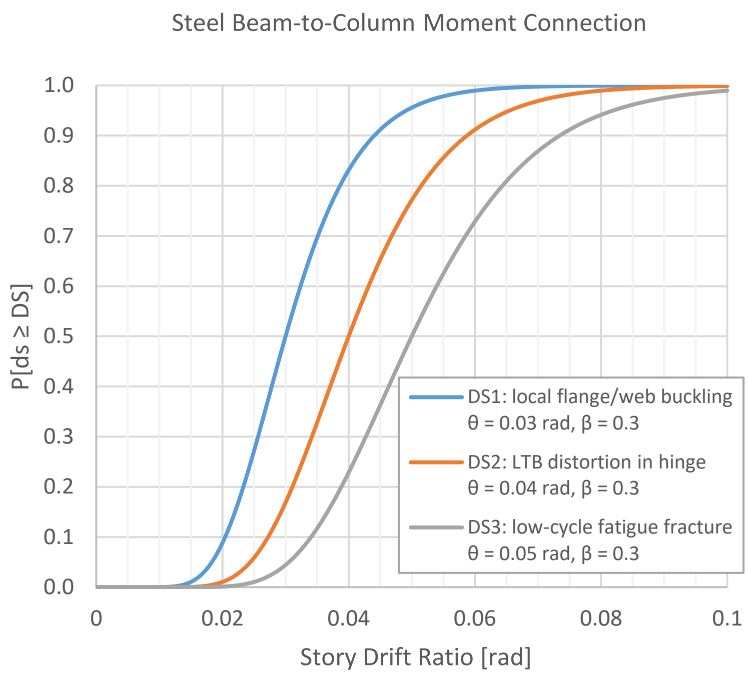


*Figure 9 – Fragility functions for steel special moment connections. Damage state details are provided in Table 5.*

### *2.2.4. Steel Gravity Connection Fragilities*

Steel gravity beam-to-column connections are based on fragility development by Deierlein and Victorsson (2008) during the FEMA P-58 Project and are available within the FEMA P-58 fragility database. The fragilities are based on thirteen experimental tests on simple bolted shear tab connections conducted by Liu and Astaneh (2000). Fragilities are developed using story drift ratio as the EDP.

Fragility functions for steel gravity connections are comprised of three sequential damage states with DS1 split into two mutually exclusive DSs to either conduct or neglect minor repairs. DS2 is assigned a Safety Class of 2, while DS3 is assigned a Safety Class of 3. The original FEMA P-58 fragilities assigned Safety Class 2 to both DS2 and DS3. Following review of the damage description for DS3, the Safety Class was increased to 3 to be more in line with the Safety Class definitions (see Table 2). A summary of the fragility functions and corresponding safety class assignments is provided in Table 6. Figure 10 shows example photographs of each damage state. A plot of the fragility functions is provided in Figure 11.

*Table 6. Bolted shear tab gravity connection fragility damage states and corresponding safety classes.*

| **Damage State**[a] | **Median (θ)**[b] | **β** | **Safety Class**[c] | **Damage Description** | **Repair Measures** |
|---|---|---|---|---|---|
| DS1a (0.95) | 4.00% | 0.4 | 0 | Yielding of shear tab and elongation of bolt holes, possible crack initiation around bolt holes or at shear tab weld. Damage in field is either obscured or deemed to not warrant repair. No repair conducted. | Careful inspection and welded repair to any cracks and possible replacement of shear tab if bolt hole deformations are excessive (possible for deeper 6-bolt or deeper shear tabs). Field condition is deemed to not warrant repair by field observation. |
| DS1b (0.05) | 4.00% | 0.4 | 0 | Yielding of shear tab and elongation of bolt holes, possible crack initiation around bolt holes or at shear tab weld. | Careful inspection and welded repair to any cracks and possible replacement of shear tab if bolt hole deformations are excessive (possible for 6-bolt or deeper shear tabs). |
| DS2 | 8.00% | 0.4 | 2 | Partial tearing of shear tab and possibility of bolt shear failure (6-bolt or deeper connections). | Repairs will include either welded repair of shear tab or possible complete replacement of shear tab and installation of new bolts. Repairs may require shoring of beam. |
| DS3 | 11.00% | 0.4 | 3[d] | Complete separation of shear tab, close to complete loss of vertical load resistance. | Repair will include complete replacement of shear tab and installation of new bolts. Repairs will require shoring of beam. |

[a] Mutually exclusive damage states (e.g., DSXa and DSXb) include the probability of occurrence in parentheses

[b] Fragility function is a lognormal distribution with median and standard deviation of θ and β, respectively. The EDP is story drift ratio.

[c] SC 1 = 50%, SC 2 = 25%, SC 3 = 10% allowable quantity of damaged components per direction per story; SC 0 does not result in SCSD.

[d] Original FEMA P-58 database assigns this damage state as Safety Class 2. This report deviates from the original FEMA P-58 database assignment to provide a more conservative Safety Class assignment.

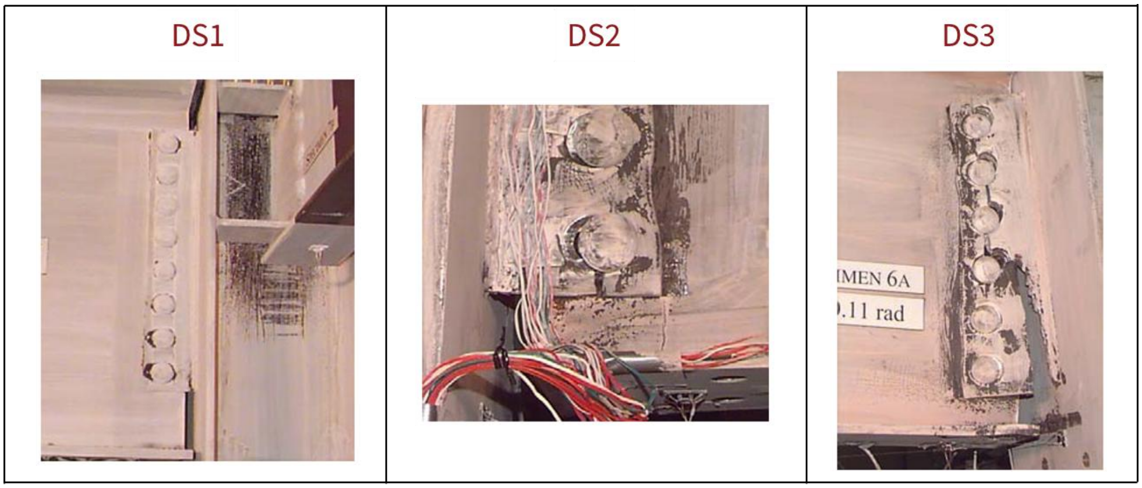


*Figure 10 – Illustration of damage states for steel shear tab connections (Deierlein and Victorsson, 2008).*

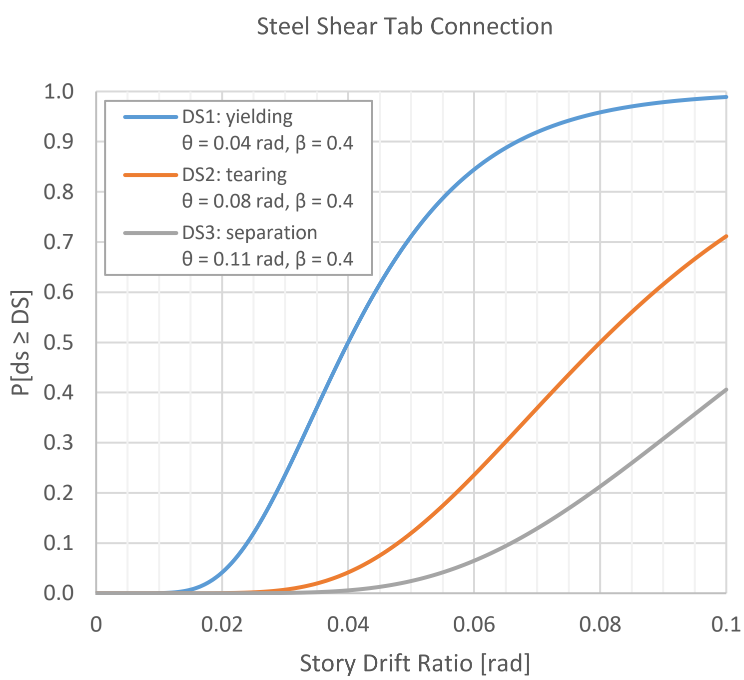


*Figure 11 – Fragility functions for bolted shear tab gravity connections. Damage state details are provided in Table 6.*

### *2.2.5. Steel Column Baseplate Fragilities*

Steel column baseplates are based on fragility development by Deierlein and Victorsson (2008) during the FEMA P-58 Project and are available within the FEMA P-58 fragility database. The fragilities are based on thirteen experimental tests on exposed column baseplates reported by three studies (Burda and Itani, 1999; Fahmy, 1999; Hajjar et al. 2005). All tests considered loading in the strong axis direction of the column. Fragilities are developed using story drift ratio as the EDP.

Fragility functions for steel column baseplate connections are comprised of three sequential damage states with DS1 split into two mutually exclusive DSs to either conduct or neglect minor repairs. DS2 is associated with crack propagation into the column or baseplate. DS3 represents the complete fracture and dislocation of the column. DS2 and DS3 are assigned Safety Classes of 2 and 3, respectively. A summary of the fragility functions is provided in Table 7. Illustrations of damage states are provided in Figure 12. A plot of the fragility functions for steel base plates is provided in Figure 13.

*Table 7. Steel column baseplate connection fragility damage states and corresponding safety classes.*

| **Damage State**[a] | **Median (θ)**[b] | **β** | **Safety Class**[c] | **Damage Description** | **Repair Measures** |
|---|---|---|---|---|---|
| DS1a (0.95) | 4.00% | 0.4 | 0 | Initiation of crack at the fusion line between the column flange and the base plate weld. Damage in field is either obscured or deemed to not warrant repair. No repair conducted. | The repair will involve removal of a portion of grade slab, gouging out material surrounding the fracture initiating and re-welding, then repair of slab. Field condition is deemed to not warrant repair by field observation. |
| DS1b (0.05) | 4.00% | 0.4 | 0 | Initiation of crack at the fusion line between the column flange and the base plate weld. | The repair will involve removal of a portion of grade slab, gouging out material surrounding the fracture initiating and re-welding, then repair of slab. |
| DS2 | 7.00% | 0.4 | 2 | Propagation of brittle crack into column and/or base plate. | Depending on the crack trajectory, the repair will range from replacement of a portion of the column or base plate to full replacement of the column base. Replacement will require shoring of column, torch cutting to remove damaged material, and fabrication and field welding to install replacement material. |
| DS3 | 10.00% | 0.4 | 3 | Complete fracture of the column (or column weld) and dislocation of column relative to the base. | Repair would likely involve replacing the entire base plate assembly and most of the column in the story above the base plate. |

[a] Mutually exclusive damage states (e.g., DSXa and DSXb) include the probability of occurrence in parentheses
[b] Fragility function is a lognormal distribution with median and standard deviation of θ and β, respectively. The EDP is story drift ratio.
[c] SC 1 = 50%, SC 2 = 25%, SC 3 = 10% allowable quantity of damaged components per direction per story; SC 0 does not result in SCSD.

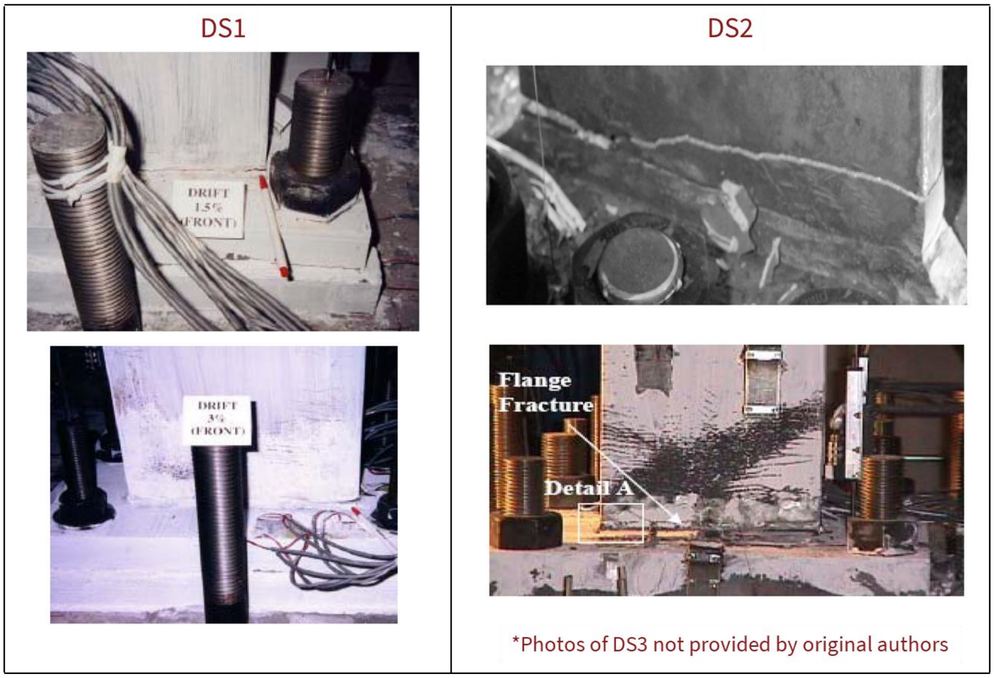


*Figure 12 – Illustration of the first two damage states for steel column baseplates (Deierlein and Victorsson, 2008).*

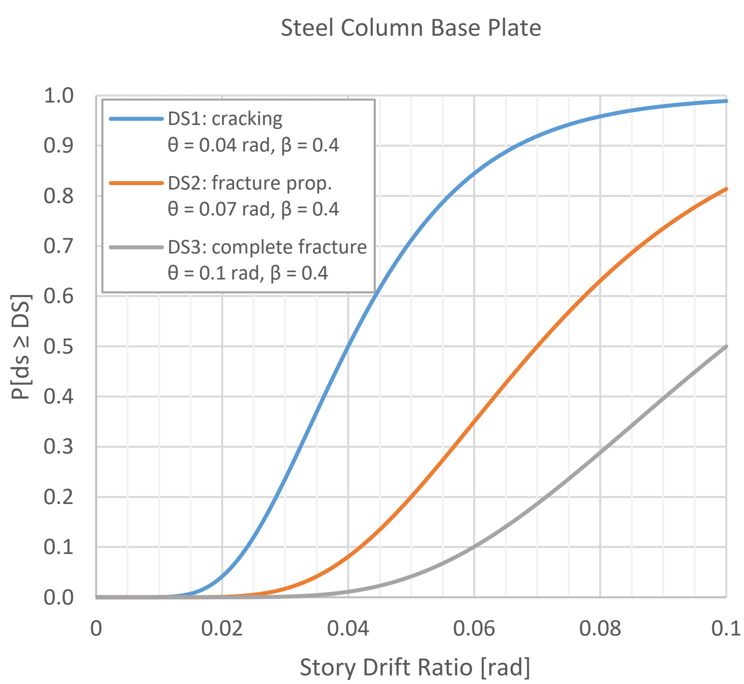


*Figure 13 – Fragility functions for steel column baseplates. Damage state details are provided in Table 7.*

### 2.2.6. Welded Column Splice Fragilities

Steel welded column splices are based on fragility development by Deierlein and Victorsson (2008) during the FEMA P-58 Project and are available within the FEMA P-58 fragility database. The fragilities are based on experimental testing conducted by Bruneau et al. (1987) and fracture analysis performed by Nuttayasakul (2001). Fragilities are developed using story drift ratio as the EDP.

Fragility functions for welded steel column splices are comprised of two sequential damage states with DS1 split into two mutually exclusive DSs to either conduct or neglect minor repairs. DS2 represents complete fracture of the splice and is attributed a Safety Class of 3. A summary of the fragility functions is provided in Table 8. A plot of the fragility functions is provided in Figure 14. Notably, original documentation for these fragilities did not provide photographs of damage states.

*Table 8. Welded column splice fragility damage states and corresponding safety classes.*

| Damage State[a] | Median (θ)[b] | β | Safety Class[c] | Damage Description | Repair Measures |
|---|---|---|---|---|---|
| DS1a (0.95) | 2.00% | 0.4 | 0 | Ductile fracture of the groove weld flange splice. Damage in field is either obscured or deemed to not warrant repair. No repair conducted. | Repair would involve gouging out the material adjacent to the fracture and repairing with a new groove weld. Field condition is deemed to not warrant repair by field observation. |
| DS1b (0.05) | 2.00% | 0.4 | 0 | Ductile fracture of the groove weld flange splice. | Repair would involve gouging out the material adjacent to the fracture and repairing with a new groove weld. |
| DS2 | 5.00% | 0.4 | 3 | DS1 followed by complete failure of the web splice plate and dislocation of the two column segments on either side of the splice. | Repair may not be practically feasible, but would require either realignment or replacement of adjacent column segments and rewelding of splice. |

[a] Mutually exclusive damage states (e.g., DSXa and DSXb) include the probability of occurrence in parentheses

[b] Fragility function is a lognormal distribution with median and standard deviation of θ and β, respectively. The EDP is story drift ratio.

[c] SC 1 = 50%, SC 2 = 25%, SC 3 = 10% allowable quantity of damaged components per direction per story; SC 0 does not result in SCSD.

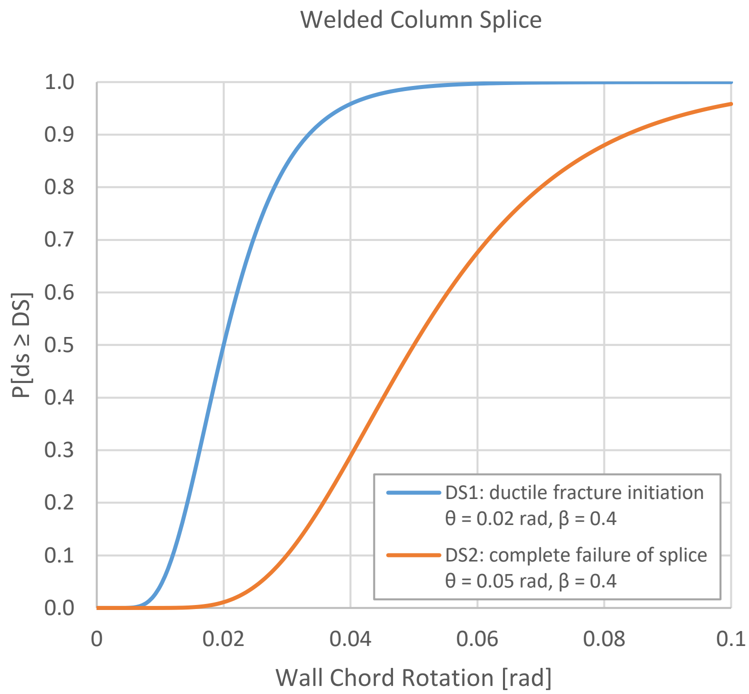


*Figure 14 – Fragility functions for welded column splices. Damage state details are provided in Table 8.*

## 2.3. Archetypes Considered for Analysis

To determine the combination of $R_{fr}$ and $\Delta_{afr}$ that results in acceptable functional recovery performance, an archetype space is broken up into performance groups, analyzed, and the overall parameters are determined by the worst-case of the performance groups. Performance groups are defined in accordance with the proposed Section A.8.3.6 procedures of the 2026 NEHRP Provisions.

The DSMF system has an archetype space comprised of three different performance groups and a total of 54 individual archetype variants. The background on the development of the archetype design space is presented in the following sub-sections.

### *2.3.1. Building Configuration and Structural Component Population*

All archetypes assume a constant plan area of 100 feet by 100 feet. Story heights are assumed to be 15 and 13 feet for the first and typical stories, respectively. These story heights were used for special (undamped) steel moment frames in previous FEMA P-695 assessments (NIST, 2010).

The following archetype variables are considered for the DSMF:

- Number of stories;
- Damper configuration;
- Damped frame bay width.

Building heights range from 2 to 20 stories, split into three height classes: low-rise (2, 3, and 4 stories), mid-rise (6, 8 and 10 stories), and high-rise (12, 16 and 20 stories). Damper configurations consider diagonal, chevron, and modified chevron with horizontal dampers (MCHD; see Figure 4). The damped frame (DF) bay length is 20 or 30 feet for all damper configurations in each principal direction. This combination of damper configuration and bay spacing produces a range of required damper strokes that directly affect the damper assembly fragility functions discussed in Section 2.2.1. The SP3 analyses do not distinguish between Type I, II, and III system types (see Figure 1); while this distinction is important for design (e.g. proportioning shared columns between the DF and the MF), it has very little impact on global strength and stiffness properties and structural response of the building.

Typical plan layouts and populated structural components for each principal direction are shown in Figure 15, depicting a Type I system configuration (see Figure 1). Steel shear tab gravity connections are assumed at every location outside of the moment frame (MF). Column base plates are populated at each base column within a MF bay. An elevation view of a 6-story archetype MF with populated structural components is shown in Figure 16. Welded column splices are populated at every second story. Moment connections are populated as either interior (beam both sides) or exterior (beam one side) assemblies.

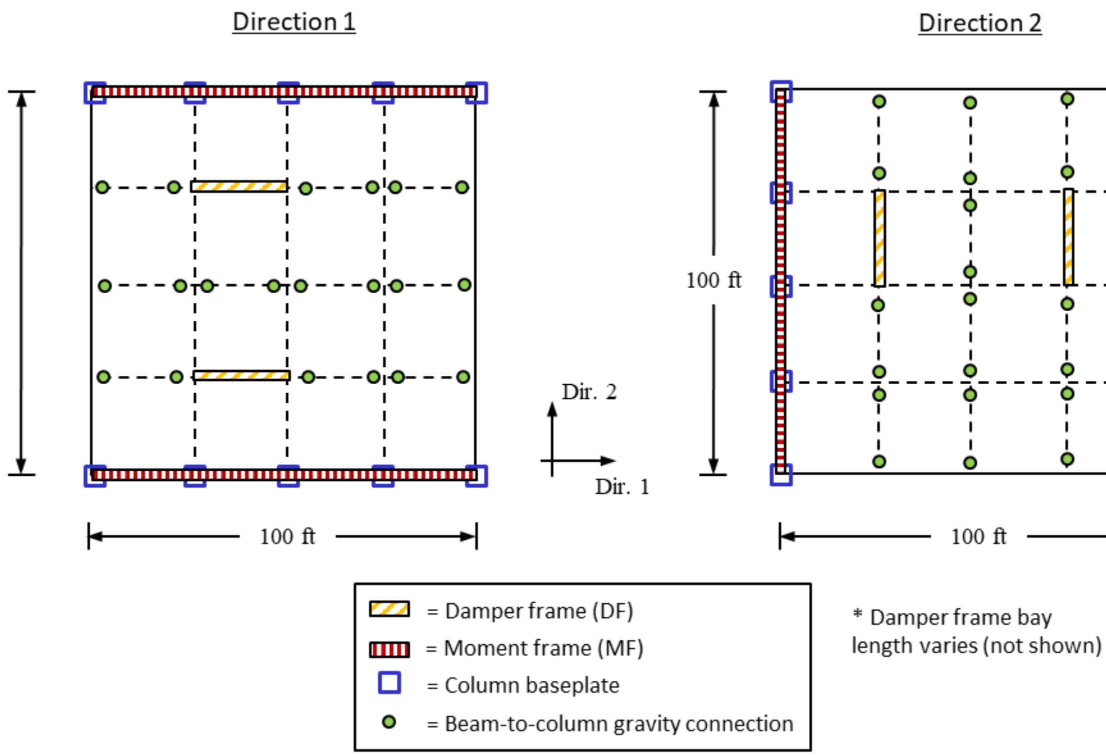


*Figure 15 – Illustration of assumed plan layouts for DSMF archetypes with population of structural components: Direction 1 (left), Direction 2 (right).*

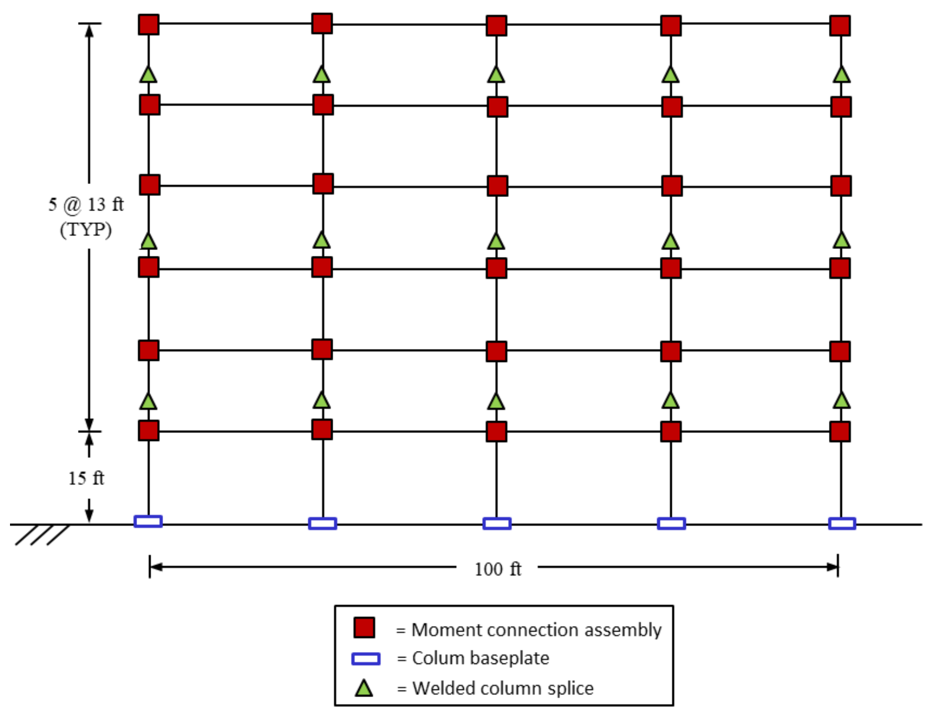


*Figure 16 – Elevation views of 6-story DSMF moment frame with populated structural components*

The SP3 analysis procedure (see Section 2.4) is based on calibration to Type I DSMF systems and does not distinguish between Type I, II and III (see Figure 1). This is due to Type I systems being the most common, and Type II and III systems having very similar global response characteristics. The main difference between Type I and Type II/III systems is that the moment frame elements must accommodate additional loading due to viscous damper forces. This results in slightly larger structural sections for beams (Type II) and columns (Type II and III) compared to what is required for a Type I moment frame. Explicit inclusion of these differences would result in slightly shorter periods and slightly increased global overstrength, but difference in response has been shown to be very minimal (Welch et al. 2023b). These slight differences are not captured in the current analysis based on Type I response, yet are applicable; excluding them is modestly conservative, for Type II and Type III systems.

### *2.3.2. Performance Groups for DSMF*

The performance groups considered were low (PG1), mid, (PG2) and high-rise (PG3) buildings of similar heights used in assessing seismic performance factors for life-safety using FEMA P-695 analysis for special (undamped) steel moment frames (NIST, 2010) and those used for AC494 qualification of the TDMF™ design procedure (Welch et al. 2023a, b). Each building height is assessed assuming three different damper configurations: chevron, diagonal, and modified chevron with horizontal dampers (MCHD). Each damper configuration assumes damped frame bays of 20 and 30 feet. The building height ranges (i.e., number of stories) and damper configurations in each performance group are shown in Table 9.

The use of building height to define (or delineate) performance groups has a strong precedence in numerous applications of the FEMA P-695 methodology, which serves as a basis of the performance group concept used in the current study and underlying NEHRP Appendix A provisions. As a minimum, performance groups are distinguished between short-period (short structures) and long-period (tall structures). Damper configuration and bay length have minimal effect on the performance of DSMF buildings, so these were not used to delineate between performance groups.

*Table 9. DSMF performance group summary*

| Performance Group | Description | No. of Stories | Damper Configuration[a] | Bay Length [ft][b] |
|---|---|---|---|---|
| PG1 | Low Rise | 2, 3, 4 | Chevron, Diagonal, MCHD | 20, 30 |
| PG2 | Mid-Rise | 6, 8, 10 | Chevron, Diagonal, MCHD | 20, 30 |
| PG3 | High-Rise | 12, 16, 20 | Chevron, Diagonal, MCHD | 20, 30 |

[a] MCHD = Modified Chevron with Horizontal Dampers; [b] bay length of the damped frame

## 2.4. Estimation of Structural Responses

The structural responses for the archetypes were determined using the SP3 Structural Response Prediction Engine (SRPE) (Cook et al. 2018). The SRPE generates a simplified linear multi-degree-of-freedom model representative of strength and stiffness requirements. A linear response is determined by modal analysis, which is then modified to account for nonlinear behavior of the system, with further modifications to account for reductions in the responses due to supplemental viscous damping. The expected nonlinear behavior is calibrated by sampling from Incremental Dynamic Analysis (IDA: Vamvatsikos and Cornell, 2002) results from high-fidelity nonlinear models of moment frame buildings with and without supplemental viscous damping.

The SRPE is used to predict peak story drift ratio demands and peak floor accelerations. Residual drifts are computed using the Steel Moment Frame residual drift model that were developed as part of the ATC-138 project (ATC, 2021).

The following sections provide an overview of the analytical basis behind the SRPE and the quantification of different Engineering Demand Parameters (EDPs), and how modifications are incorporated to account for reduction in response due to supplemental viscous damping. This section focuses on the prediction of median response conditioned on spectral acceleration (Sa); record-to-record uncertainty and modeling uncertainty are modeled according to FEMA P-58 (FEMA, 2018b).

### *2.4.1. Analytical Basis Behind the Moment Frame SRPE in SP3*

The Moment Frame SRPE in SP3 is based on calibration to a subset of 30 ductile (Haselton and Deierlein, 2007; Haselton et al. 2011b) and 26 non-ductile (Liel and Deierlein, 2008; Liel et al. 2011) reinforced concrete (RC) moment frame building archetypes ranging from 1 to 20 stories in height, which were previously used in the initial development of the FEMA P-695 (FEMA, 2009) methodology for quantifying performance factors for life-safety (Liel et al. 2009; Haselton et al. 2011a). Table 10 summarizes the ductile RC moment frames used in initial SRPE calibration.

The method was later verified for use with steel moment frames using results from a subset of "baseline" nonlinear steel moment frame models that were developed for the FEMA P-2012 project (FEMA, 2018c), with heights of 3, 9, and 20 stories. Modifications to the Moment Frame SRPE in SP3 to account for supplemental damping in steel moment frame buildings are based on a subset of 12 nonlinear models that were used for qualifying the DSMF system (Welch and DeBock, 2023, Welch et al. 2023a,b), summarized in Table 11; these were analyzed using incremental dynamic analysis with and without supplemental damping included in the models, in order to understand the effect of supplemental damping over a range of shaking intensities.

Nonlinear building models for developing the moment frame SRPE, validating its use for steel moment frames, and modifying it to account for supplemental damping, were all modeled in 2D with OpenSees (McKenna et al. 2010), using nonlinear elements calibrated to experimental databases (Haselton et al. 2016; NIST, 2017). All models were analyzed using the FEMA P-695 far-field ground motion set (FEMA, 2009) consisting of 44 ground motions (i.e., 22 horizontal pairs). Incremental Dynamic Analysis (IDA: Vamvatsikos and Cornell, 2002) was used to obtain a range of linear and nonlinear structural responses for calibration.

*Table 10. Summary of building models used for calibration of the Special Moment Frame SRPE. Table adapted from Haselton et al. (2011b).*

| ID | No. Stories | Framing | Design Case | ID (cont'd) | No. Stories | Framing | Design Case |
|---|---|---|---|---|---|---|---|
| 2061 | 1 | Space | Baseline[a] | 1022 | 8 | Space | Uniform |
| 2062 | 1 | Space | Pinned | 2065 | 8 | Space | WS-1 (65%)[d] |
| 2063 | 1 | Space | Fixed | 2066 | 8 | Space | WS-1 (80%) |
| 2069 | 1 | Perimeter | Baseline | 1023 | 8 | Space | WS-2 (80%) |
| 1001 | 2 | Space | Baseline | 1024 | 8 | Space | WS-2 (65%) |
| 1001a | 2 | Space | Pinned | 1013 | 12 | Perimeter | Baseline |
| 1002 | 2 | Space | Fixed | 1014 | 12 | Space | Baseline |
| 2064 | 2 | Perimeter | Baseline | 1015 | 12 | Space | Uniform |
| 1003 | 4 | Perimeter | Baseline | 2067 | 12 | Space | WS-1 (65%) |
| 1004 | 4 | Perimeter | Uniform[b] | 2068 | 12 | Space | WS-1 (80%) |
| 1008 | 4 | Space | Baseline | 1017 | 12 | Space | WS-2 (80%) |
| 1009 | 4 | Perimeter | $L_{bay}$ = 30 ft[c] | 1018 | 12 | Space | WS-2 (65%) |
| 1010 | 4 | Space | $L_{bay}$ = 30 ft | 1019 | 12 | Space | $L_{bay}$ = 30 ft |
| 1011 | 8 | Perimeter | Baseline | 1020 | 20 | Perimeter | Baseline |
| 1012 | 8 | Space | Baseline | 1021 | 20 | Space | Baseline |

[a] Baseline design case considers rotational stiffness of grade beams and any basement stories. Pinned and fixed alternatives adjust what is assumed in design.

[b] Conservative design with constant member sizes and reinforcement over building height

[c] Baseline designs have 20 ft bay spacing, alternates have 30 ft bay spacing

[d] WS-1 is for designs with only the first story being weak, and WS-2 is for the 1st and 2nd stories being weak. Percentage is that of strength between the weakened stories and the story above.

Models used for investigating the effects of supplemental damping were developed in accordance with ATC-114/NIST modeling guidelines for steel moment frames (NIST, 2017) and included more recent relationships for the modeling of steel columns (Lignos et al. 2019) and panel zones (Skiadopoulos et al., 2021) based on the results of experimental testing. These updates specifically targeted enhancements of existing modeling relationships contained in the ATC-114/NIST guidelines (Krawinkler, 1978; Gupta and Krawinkler, 1999; Lignos and Krawinkler, 2011). Damper assemblies used a built-up Maxwell model approach and were verified to give expected dynamic response in terms of stiffness and energy dissipation characteristics compared to state-of-the art models for viscous dampers (Akcelyan et al. 2016; Akcelyan, 2017). An illustration of the modeling used for steel moment frames with supplemental damping (all Type I systems) is shown in Figure 17.

*Table 11. Summary of building models used for calibrating the effect of supplemental damping for the Special Moment Frame SRPE (Welch et al. 2023a).*

| No. Stories | Seismic Design Category (SDC) | Risk Category | MF Beam Connection | MF Column Depth | Doubler Plates |
|---|---|---|---|---|---|
| 4 | $D_{max}$ | II | RBS | W14 | yes |
| 4 | $D_{max}$ | II | WUF-W | W14 | no |
| 4 | $D_{max}$ | IV | WUF-W | W27 | no |
| 4 | E | IV | WUF-W | W36 | no |
| 8 | $D_{max}$ | II | RBS | W14 | no |
| 8 | $D_{max}$ | II | RBS | W14 | yes |
| 8 | $D_{max}$ | II | WUF-W | W14 | no |
| 12 | $D_{max}$ | II | RBS | W14 | yes |
| 12 | $D_{max}$ | IV | RBS | W36 | yes |
| 12 | $D_{max}$ | II | WUF-W | W14 | no |
| 12 | $D_{max}$ | IV | WUF-W | W36 | yes |
| 12 | E | IV | RBS | W36 | yes |

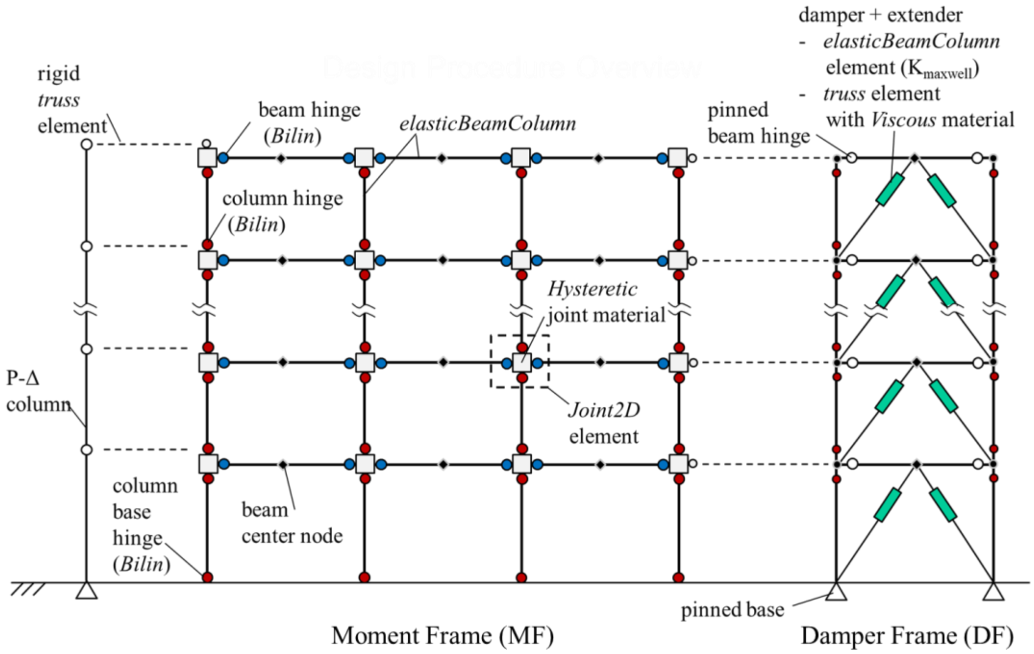


*Figure 17 – Illustration on nonlinear modeling used to calibrate the effect of supplemental damping in the Special Moment Frame SRPE (Welch et al. 2023a)*

### *2.4.2. Structural Properties Estimation*

Building structural properties are estimated using a linear building model, with strength and stiffness scaled to meet corresponding design requirements. For the DSMF system, this process incorporates the simplified seismic design criteria developed specifically for the DSMF system (ICC-ES, 2023). Typical levels of overstrength (e.g., due to expected material properties, etc.) are added after design requirements are satisfied, to provide the best possible estimate of the true strength and stiffness of the LFRS. The commercial version of SP3 also includes additional strength and stiffness contributions from the gravity system and nonstructural components, but these are excluded in this study for compliance with the procedures of section A.8.3.6 of the 2026 National Earthquake Hazards Reduction Program (NEHRP) Provisions.

The process begins by specifying the design parameters, including spectral values, response modification factor (R), deflection amplification factor ($C_d$), and related values (e.g., $I_e$). Next, a target seismic design drift is selected. For drift-controlled systems, such as most moment frames, this target is typically the design drift limit—for example, 2% for risk category II buildings. For strength-controlled systems, the target drift is a realistic value appropriate for the system type and building height; the expected design drift values are based on a database of hundreds of building designs (from archetype buildings in the SP3 SRPE database). Functional recovery design iterations use the same process with pairs of $R_{fr}$ and $\Delta_{afr}$ for a given analysis. Notably, the deflection amplification factor ($C_d$) for DSMF buildings is taken as 55% of $R_{fr}$ to account for 45% reduction in the response due to 25% supplemental damping; this is consistent with the $C_d$ =

$R_{fr}$ design philosophy of Appendix A of the 2026 NEHRP provisions, because the difference between $C_d = R_{fr}$ is due solely to supplemental damping effects. Additionally, the design base shear is reduced 25% to account for supplemental damping, in accordance with the DSMF design procedure. The importance factor ($I_e$) is taken as unity per Section A.8.3.6 of the 2026 NEHRP Provisions.

Following this, the period of a representative design model (limited to the lateral force-resisting system, or LFRS) is determined, considering the target seismic drift and stability requirements (ASCE 7-22 Section 12.8.7). This involves constructing a simple multi-degree-of-freedom (MDOF) model that reflects the system's mass and stiffness characteristics. For instance, moment frames tend to be more shear-dominated, whereas walls and braced frames are more flexure-dominated. This approach is based on a method developed by Miranda (1999) and Miranda and Reyes (2002) but utilizes matrix structural analysis—with mass and stiffness matrices—rather than purely analytical equations; it also incorporates the ability to model rotational flexibility at the base.

Starting with very low stiffness, the stiffness matrix is systematically scaled (i.e., increased) until the model achieves the target drift or less, while also satisfying stability requirements. Generally, modal response spectrum analysis (MRSA) is used to generate structural properties for buildings that are modern code-compliant, taller than four stories, and located in high or very high seismic areas. For other cases, the equivalent lateral force (ELF) procedure is used. For the DSMF system, MRSA is used for all cases, including buildings four stories and shorter, as required by the simplified linear design procedure for the DSMF system. Wind drift checks can be included in this step but were omitted for this study.

Next, the expected strength and stiffness of the LFRS are determined, accounting for overstrength. These properties vary depending on the LFRS type and building height and are calibrated using results from OpenSees models and engineering judgment. An additional optional check can be performed to ensure compatibility between strength and stiffness. If the stiffness is found to be too low in relation to the strength and yield drift, it is increased to a reasonable level.

The final estimates of the first three periods and mode shapes of the building are determined by performing an eigen analysis with the stiffness matrix and mass matrix. The final estimate of the ultimate base shear strength is determined from design strength and the expected overstrength.

For the DSMF system, the calculation of the required damper strokes is conducted directly as part of the design automation process, which is used to select the appropriate fragility functions representing the viscous damper assemblies (see Section 2.2.1). Sizing is based on input bay geometry and damper configuration (e.g., chevron or diagonal). The required damper stroke is converted to an equivalent story drift ratio that is used to define the medians for viscous damper fragility functions.

### 2.4.3. *Story Drift Ratio*

The Moment Frame SRPE estimates peak story drift ratio at each story, accounting for the first three mode shapes and periods of the building and its peak strength. First, peak roof drift ratio is estimated using a method that is similar to the ASCE 41 (ASCE, 2023) method for target roof displacement (Section 7.4.3.3.2), but with factors calibrated directly to the OpenSees model results; it depends on the fundamental building period, modal participation factor, spectral acceleration, and correction factors for nonlinear behavior. Second, linear modal analysis is performed using the first three modes, and the results are scaled so that the roof drift from the first step is reproduced. If the spectral acceleration demand is large enough to cause yielding in the structure, then the story drifts are adjusted to account for nonlinear demands. Nonlinear demands are adjusted based on an intensity factor $S = S_a/(V_{max}/W)$, where $S_a$ is the first mode spectral acceleration and $(V_{max}/W)$ represents the normalized peak strength of the building using expected properties. Larger values of S (i.e. more damage) result in more drift concentration in the lower stories. The way in which drifts localize as S increases is calibrated to the nonlinear modeling results and depends on the height of the building (i.e., number of stories). An example calibration for a 12-story RC special moment frame model is shown in Figure 18. The solid lines represent the median peak drift profile from nonlinear time history analysis (NRHA) compared to SRPE response shown in thicker dashed lines. The dotted lines show the elastic response profile before adjusting for nonlinear behavior.

For DSMF buildings, peak roof drift ratio and the intensity factor $S = S_a/(V_{max}/W)$ that is used to determine drift concentrations are reduced to account for supplemental damping consistent with the observed response of the damped frame models that are the basis for the calibration. All other aspects of the Moment Frame SRPE are unchanged. The level of reduction depends on the damping ratio at the intensity of interest. The damping ratio at a given intensity assumes that the damping system is designed to have a damping ratio of 0.25 at the DE intensity, and that dampers have a nonlinear velocity exponent of 0.4, as required by the DSMF design procedure. Due to the nonlinear behavior of dampers (velocity exponent less than 1.0), damping ratios at intensities larger than the DE are less than 0.25, and damping ratios for intensities smaller than the DE are more than 0.25. The reduction in response due to damping matches very closely with the theoretical reduction one would compute for the first mode response.

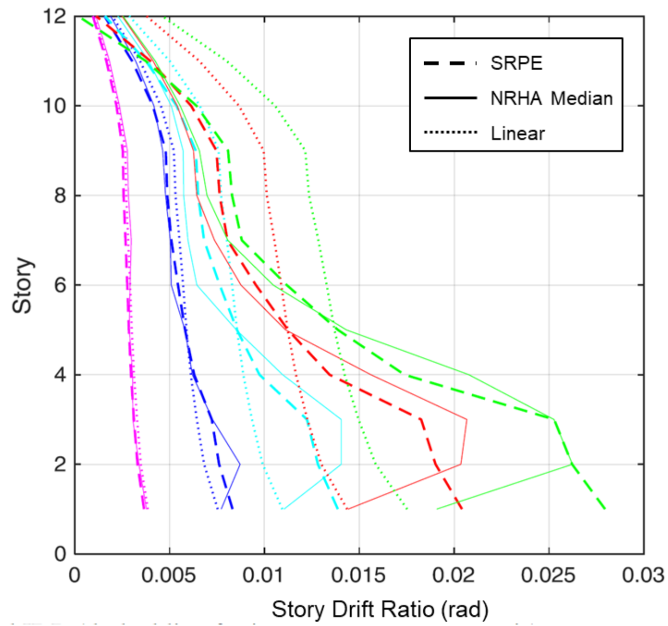


*Figure 18. Comparison of SRPE (dashed) and median NRHA (solid) story drift ratio response for a 12-story RC special moment frame. Note, dotted lines represent predicted linear response prior to adjustment for nonlinear behavior. Figure adapted from Cook et al. (2018).*

### *2.4.4. Peak Floor Acceleration*

Peak floor acceleration (PFA) is computed based on spectral acceleration, building strength, and the first three modal periods and shapes of the building. First, elastic PFA is computed with modal time-history analysis using the FEMA P-695 far-field record set scaled to the intensity of interest. Then, if the spectral acceleration demand is large enough to cause yielding, PFA is adjusted using the intensity factor $S = S_a/(V_{max}/W)$. The amount of adjustment of the response depends on how high the story is above the ground, because damage in the lower stories "isolates" the upper stories from acceleration input. An example calibration for a 12-story RC special moment frame model is shown in Figure 19. The solid lines represent the median PFA profile from NRHA compared to SRPE response shown in thicker dashed lines. The dotted lines show the elastic response profile before adjusting for nonlinear behavior. Note that the largest intensity shaking (green lines) has significant reductions in PFA at upper stories due to damage in the lower stories.

For DSMF buildings, the PFA estimation is obtained from the Moment Frame SRPE, but then reduced to account for supplemental damping. Reductions in PFA depend on the floor level under consideration; the largest PFA reduction occurs at the roof level, and there is zero PFA reduction at the ground level; reductions at intermediate stories are obtained by interpolation

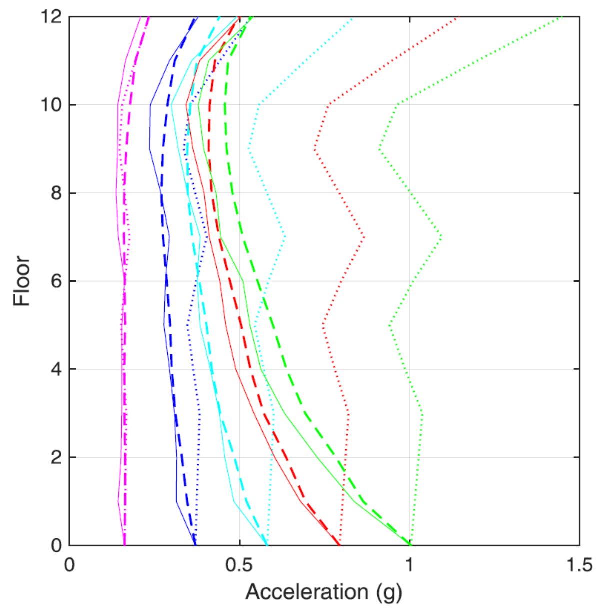


*Figure 19. Comparison of SRPE (dashed) and median NRHA (solid) peak floor acceleration response for a 12-story RC special moment frame. Note, dotted lines represent predicted linear response prior to adjustment for nonlinear behavior. Figure adapted from Cook et al. (2018).*

.

### *2.4.5. Residual Drift Ratio*

The FEMA P-58 residual drift modeling was updated during the ATC-138 project (ATC, 2021) and resulted in a supplemental FEMA P-58 background document *BD 3.7.26: Updated Model and Criteria for Residual Drift* (DeBock et al. 2024). The revisions to the original FEMA P-58 model allowed for distinctions between structural systems, based on recent analytical studies (Almeter et al. 2018; Vouvakis Manousakis et al. 2024).

The median residual story drift ratio ($\Delta_r$) is estimated from the median transient story drift ratio ($\Delta$) and yield drift ratio ($\Delta_y$). The general format for simplified residual drift estimation has a trilinear form with a transition slope and a primary slope. The initial slope represents the elastic response range (i.e., $\Delta \leq \Delta_y$) where residual displacement is not expected. The transition slope reduces the rate of residual drift accumulation in the region just beyond elastic response to a specified drift ductility, after which, the steeper primary slope accumulates residual drift at a faster rate as peak drift demands increase. The end of the transition region is defined by a system specific drift value $\Delta_{shift}$. An illustration of the basic components of the trilinear residual drift model is shown in Figure 20.

Three residual drift models were developed as part of the FEMA P-58 revisions, with parameters summarized in

Table 12. For the DSMF system, the Steel MRF model is selected according to the FEMA P-58 recommendations, listed in Table 13. The recommended yield drift ratio ($\Delta_y$) of 1.0% is also taken from Table 13. The residual story drift ratio as a function of story drift ratio demand for the DSMF system is shown in Figure 21.

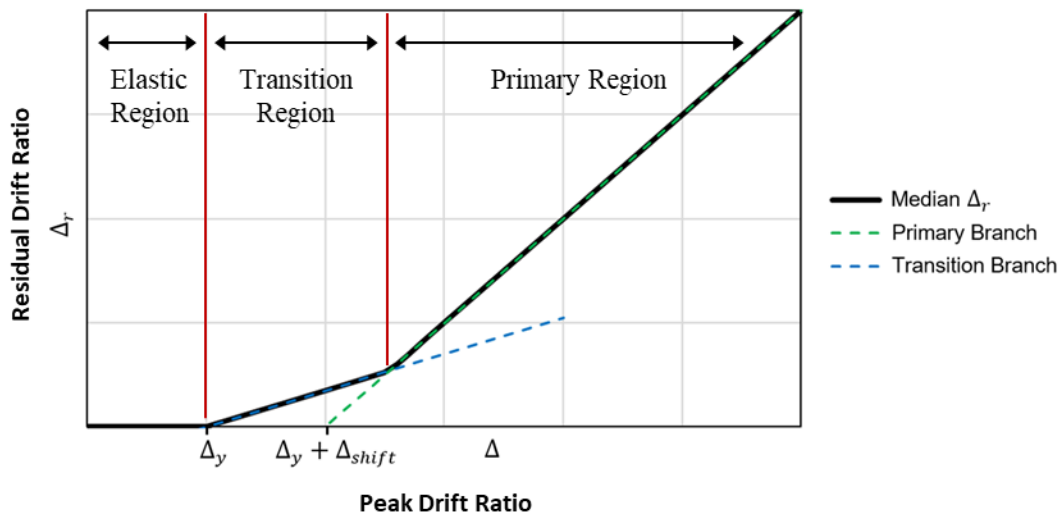


*Figure 20 – Basic components of the trilinear model to estimate residual story drift as a function of peak story drift demand and yield story drift.*

*Table 12. Parameters of updated FEMA P-58 residual drift models*

| **Residual Drift Model** | $\Delta_{shift}$ | **Primary Slope (a)** | **Transition Slope (b)** |
|---|---|---|---|
| Steel MRF | 0.005 | 0.5 | 0.2 |
| BRBF | 0.007 | 0.4 | 0.1 |
| General Inelastic | 0.008 | 0.35 | 0.15 |

*Table 13. Recommended yield story drift ratio ($\Delta_y$) and residual drift models by LFRS*

| **LFRS** | **$\Delta_y$ (rad)** | **Residual Drift Model** |
|---|---|---|
| Steel MRF | 0.01 | Steel MRF |
| Steel CBF | 0.003 | General Inelastic |
| Steel EBF | 0.005 | BRBF |
| Steel BRBF | 0.002 | BRBF |
| RC MF | 0.0075 | General Inelastic |

| | | |
|---|---|---|
| RC Wall | 0.0025 | General Inelastic |
| Masonry | 0.0025 | General Inelastic |
| Wood or CFS light frame | 0.075 | General Inelastic |

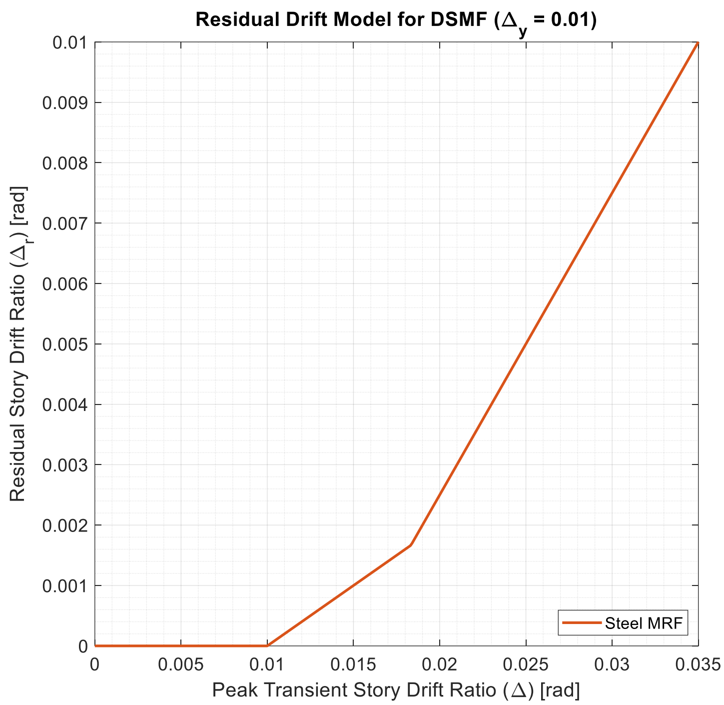


*Figure 21. Residual drift model for the DSMF structural system*

## 3. RESULTS

The tables and plots below show the Rfr and Δafr envelope for each performance group variant combination. This design envelope identifies the possible design value combinations where all performance groups satisfy both the max and mean analysis criteria. Results are provided separately for both FRC A/B/C acceptance criteria in Sections 3.2 and 3.2 and FRC D acceptance criteria in Section 3.4. Additional figures that illustrate general system performance in terms of structural response, controlling component damage and controlling design features are provided in Section 3.5. Section 3.4 then contains the results of verification checks for peak floor acceleration demands. Full details on the performance of individual archetypes are also provided in the attached supplementary materials.

## 3.1. FRC A/B/C Analysis Results (with Fixed Beam-to-Column Connections in Damper Frame, Including Gusset Damageability)

*Table 14 – $R_{fr}$ values across various allowable drift limits required to satisfy the FRC A/B/C structural performance acceptance criteria for each performance group (for fixed beam-to-column connections in damper frame).*

| Performance Group | Criteria | $\Delta_{afr}$ | | | | | | |
|---|---|---|---|---|---|---|---|---|
| | | 0.005 | 0.0075 | 0.01 | 0.0125 | 0.015 | 0.0175 | 0.02 |
| PG1-DSMF | Max[1] | 8 | 8 | 8 | 8 | 8 | 8 | 8 |
| PG2-DSMF | Max[1] | 8 | 8 | 8 | 8 | 8 | 8 | 8 |
| PG3-DSMF | Max[1] | 8 | 8 | 8 | 8 | 8 | 8 | 8 |
| PG1-DSMF | Mean[1] | 8 | 8 | 8 | 8 | 8 | 8 | 8 |
| PG2-DSMF | Mean[1] | 8 | 8 | 8 | 6.0 | 5.5 | 5.5 | 5.5 |
| PG3-DSMF | Mean[1] | 8 | 8 | 8 | 8 | 8 | 8 | 8 |
| | **Envelope** | 8 | 8 | 8 | 8 | 8 | 8 | 8 |

[1]In each performance group, the combination of $R_{fr}$ and $\Delta_{afr}$ is deemed to be acceptable if the mean P[SCSD] is less than 10%, and the maximum P[SCSD] across all archetypes in the performance group is less than 20%.

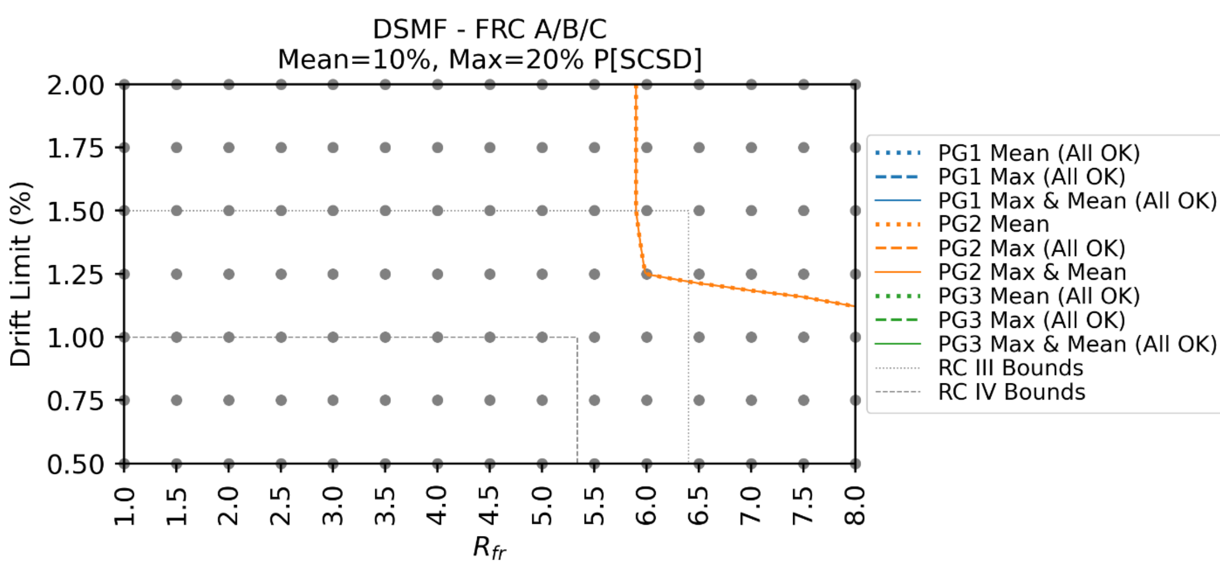


*Figure 22 – Combination of $R_{fr}$ and $\Delta_{afr}$ values required to satisfy the FRC A/B/C structural performance acceptance criteria for each performance group (for fixed beam-to-column connections in damper frame).*

### 3.2. FRC A/B/C Analysis Results (with Pinned Beam-to-Column Connections in Damper Frame, Excluding Gusset Damageability)

*Table 15 – $R_{fr}$ values across various allowable drift limits required to satisfy the FRC A/B/C structural performance acceptance criteria for each performance group (for pinned beam-to-column connections in damper frame).*

| Performance Group | Criteria | $\Delta_{afr}$ 0.005 | 0.0075 | 0.01 | 0.0125 | 0.015 | 0.0175 | 0.02 |
|---|---|---|---|---|---|---|---|---|
| PG1-DSMF | Max[1] | 8 | 8 | 8 | 8 | 8 | 8 | 8 |
| PG2-DSMF | | 8 | 8 | 8 | 8 | 8 | 8 | 8 |
| PG3-DSMF | | 8 | 8 | 8 | 8 | 8 | 8 | 8 |
| PG1-DSMF | Mean[1] | 8 | 8 | 8 | 8 | 8 | 8 | 8 |
| PG2-DSMF | | 8 | 8 | 8 | 8 | 8 | 8 | 8 |
| PG3-DSMF | | 8 | 8 | 8 | 8 | 8 | 8 | 8 |
| | **Envelope** | 8 | 8 | 8 | 8 | 8 | 8 | 8 |

[1]In each performance group, the combination of $R_{fr}$ and $\Delta_{afr}$ is deemed to be acceptable if the mean P[SCSD] is less than 10%, and the maximum P[SCSD] across all archetypes in the performance group is less than 20%.

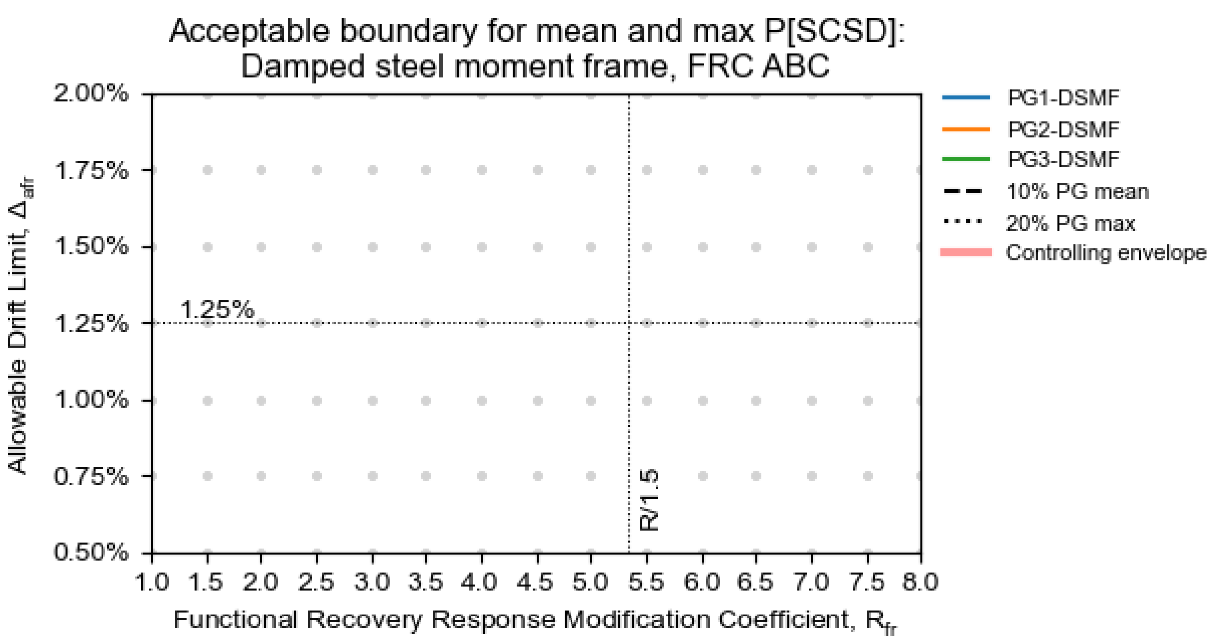


*Figure 23 – Combination of $R_{fr}$ and $\Delta_{afr}$ values required to satisfy the FRC A/B/C structural performance acceptance criteria for each performance group (for pinned beam-to-column connections in damper frame; 10% P[SCSD] envelope is outside the bounds of this plot, so nothing is shown).*

### 3.3. FRC D Analysis Results (with Fixed Beam-to-Column Connections in Damper Frame, Including Gusset Damageability)

*Table 16 – $R_{fr}$ values across various allowable drift limits required to satisfy the FRC D structural performance acceptance criteria for each performance group (for fixed beam-to-column connections in damper frame).*

| Performance Group | Criteria | $\Delta_{afr}$ 0.005 | 0.0075 | 0.01 | 0.0125 | 0.015 | 0.0175 | 0.02 |
|---|---|---|---|---|---|---|---|---|
| PG1-DSMF | Max[1] | 8 | 8 | 8 | 8 | 8 | 8 | 8 |
| PG2-DSMF | | 8 | 8 | 8 | 8 | 8 | 8 | 8 |
| PG3-DSMF | | 8 | 8 | 8 | 8 | 8 | 8 | 8 |
| PG1-DSMF | Mean[1] | 8 | 8 | 8 | 8 | 8 | 8 | 8 |
| PG2-DSMF | | 8 | 8 | 8 | 8 | 8 | 8 | 8 |
| PG3-DSMF | | 8 | 8 | 8 | 8 | 8 | 8 | 8 |
| | **Envelope** | 8 | 8 | 8 | 8 | 8 | 8 | 8 |

[1] In each performance group, the combination of $R_{fr}$ and $\Delta_{afr}$ is deemed to be acceptable if the mean P[SCSD] is less than 15%, and the maximum P[SCSD] across all archetypes in the performance group is less than 25%.

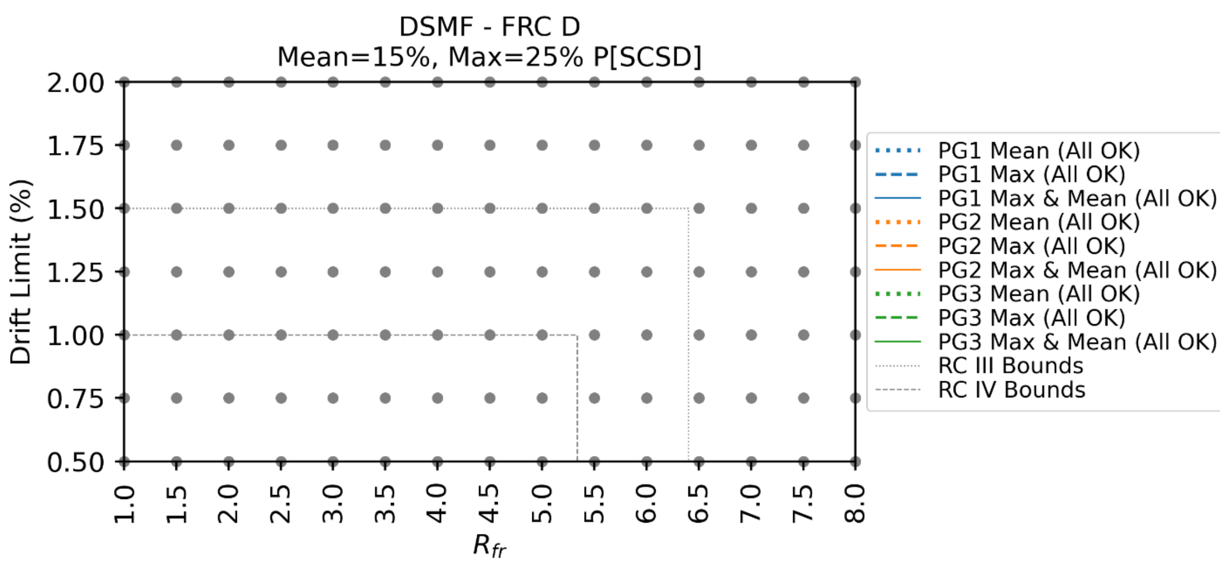


*Figure 24 – Combination of $R_{fr}$ and $\Delta_{afr}$ values required to satisfy the FRC D structural performance acceptance criteria for each performance group (for fixed beam-to-column connections in damper frame;15% P[SCSD] envelope is outside the bounds of this plot, so nothing is shown).*

## 3.4. FRC D Analysis Results (with Pinned Beam-to-Column Connections in Damper Frame, Excluding Gusset Damageability)

*Table 17 – $R_{fr}$ values across various allowable drift limits required to satisfy the FRC D structural performance acceptance criteria for each performance group (for pinned beam-to-column connections in damper frame).*

| Performance Group | Criteria | $\Delta_{afr}$ 0.005 | 0.0075 | 0.01 | 0.0125 | 0.015 | 0.0175 | 0.02 |
|---|---|---|---|---|---|---|---|---|
| PG1-DSMF | Max[1] | 8 | 8 | 8 | 8 | 8 | 8 | 8 |
| PG2-DSMF | | 8 | 8 | 8 | 8 | 8 | 8 | 8 |
| PG3-DSMF | | 8 | 8 | 8 | 8 | 8 | 8 | 8 |
| PG1-DSMF | Mean[1] | 8 | 8 | 8 | 8 | 8 | 8 | 8 |
| PG2-DSMF | | 8 | 8 | 8 | 8 | 8 | 8 | 8 |
| PG3-DSMF | | 8 | 8 | 8 | 8 | 8 | 8 | 8 |
| | **Envelope** | 8 | 8 | 8 | 8 | 8 | 8 | 8 |

[1]In each performance group, the combination of $R_{fr}$ and $\Delta_{afr}$ is deemed to be acceptable if the mean P[SCSD] is less than 15%, and the maximum P[SCSD] across all archetypes in the performance group is less than 25%.

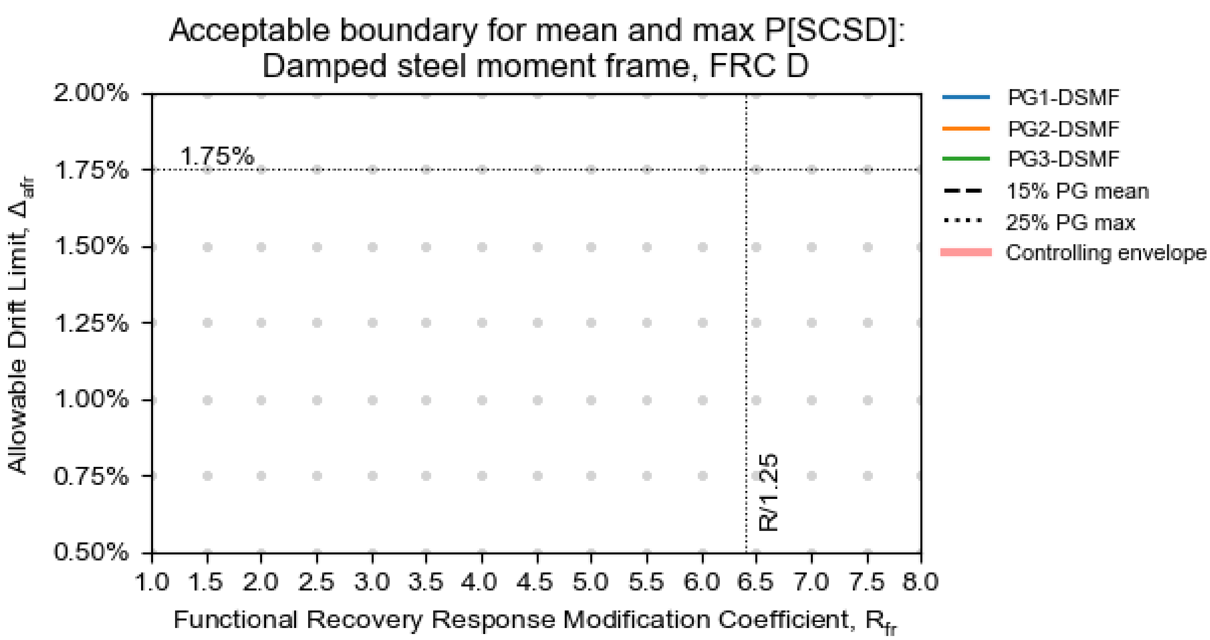


*Figure 25 – Combination of $R_{fr}$ and $\Delta_{afr}$ values required to satisfy the FRC D structural performance acceptance criteria for each performance group (for pinned beam-to-column connections in damper frame;15% P[SCSD] envelope is outside the bounds of this plot, so nothing is shown).*

### 3.5. System Response

The figures below provide detailed insights into the general response and performance outcomes of the models making up each performance group. Figure 26 shows how design drift ($\Delta_{afr}$) relates to median realized drift (x-axis), and how realized drift relates to P[SCSD] (y-axis). The median realized drift is the median peak story drift, in a given story, from all the realizations of peak story drift (~2,000) simulated as part of the FEMA P-58 Monte Carlo assessment. Figure 27 further breaks down the contributions of SCSD by structural component type, and shows that damper and moment connection damage are dominant in many of the performance results for DSMF buildings. Finally, Figure 28 shows when the building design transitions from strength-controlled to stiffness-controlled for various $R_{fr}$ and $\Delta_{afr}$ combinations. All results presented in this section are general to the response of the system and not specific to Functional Recovery Category.

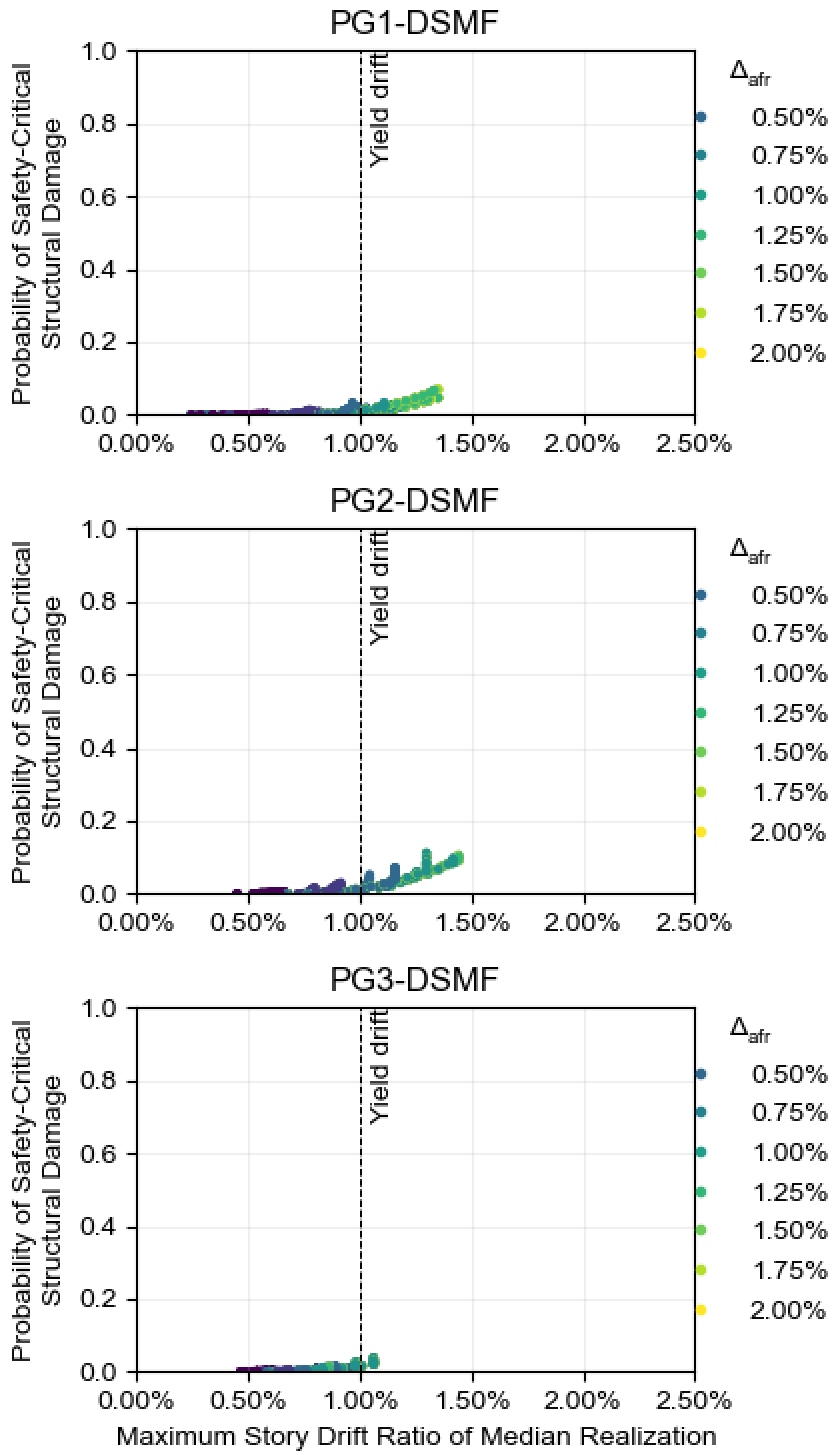


*Figure 26 - Relationship between peak realized drift (median) and P[SCSD] for all archetypes.*

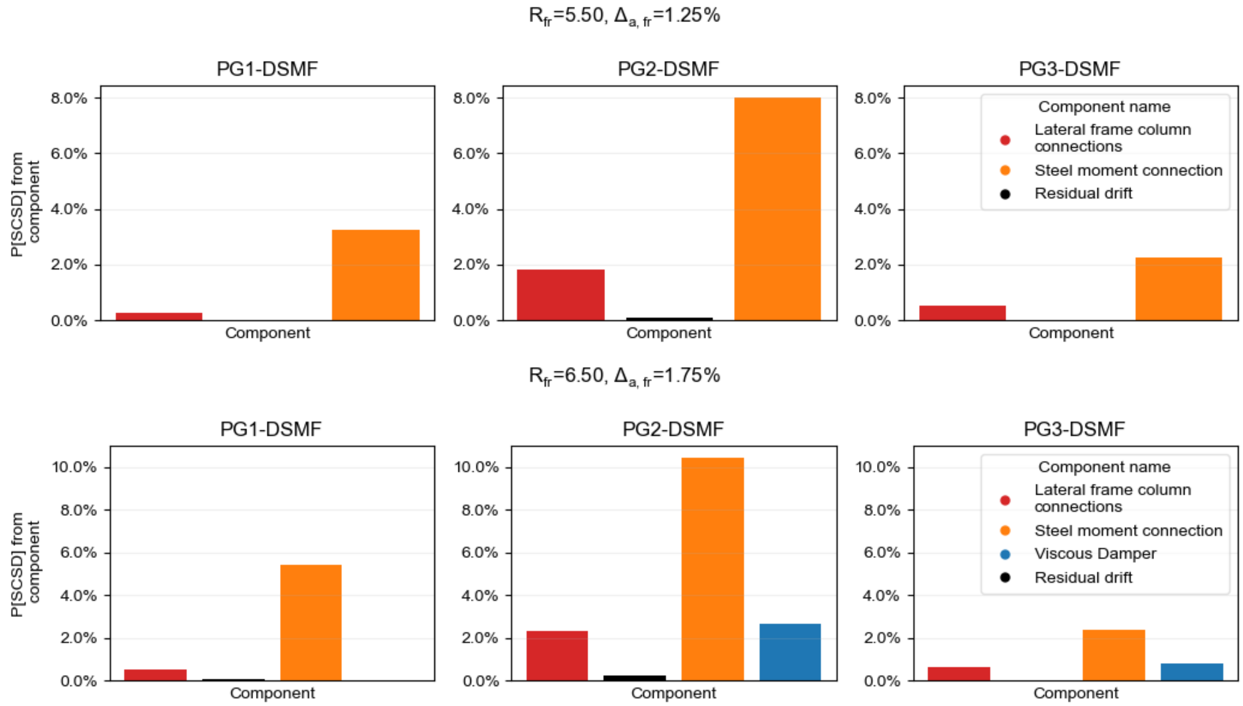


*Figure 27 – Component damage contribution to P[SCSD] for each performance group at the recommended design points for each FRC-system combination*

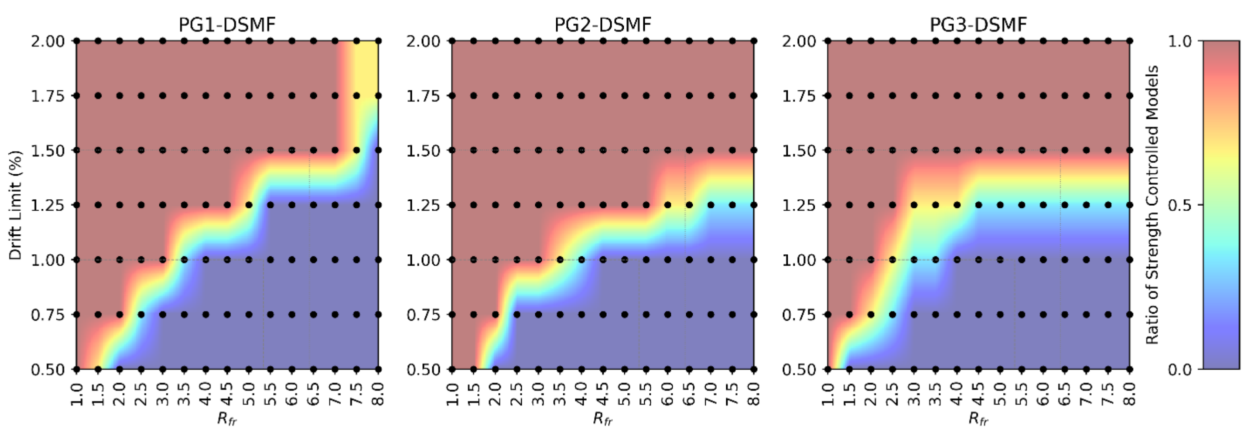


*Figure 28 – The average influence of strength on building stiffness for various design requirement combinations assessed. Red coloring indicates that 100% of the models at this design point are controlled by strength requirements (e.g., tightening drift limits by one increment will not change performance). Alternately, blue coloring indicates that 100% of the models at this design point are controlled by stiffness requirements*

### 3.6. Validation of Peak Floor Acceleration Demand Estimates

The NEHRP Provisions Appendix A Section A.8.3.6 requires that the peak floor acceleration demands be evaluated for all of the structural system archetype design cases, to ensure that the Section A.10.6 peak floor acceleration adequately reflect the actual peak floor acceleration values observed in the nonlinear response-history analysis results. The Section A.8.3.6 check then requires the $R_{\mu fr}$ value to be reduced if it is necessary to adequately predict the peak floor acceleration demands when using the Section A.10.6 equation.

This Section A.8.3.6 evaluation was completed, resulting in the following $R_{\mu fr}$ requirements:

- $R_{\mu fr} = 1.42$ is required for FRC A/B/C (based on design using $R_{fr} = 5.5$ and $\Delta_{afr} = 1.25\%$), which is identical to the baseline value (so no change required).
- $R_{\mu fr} = 1.55$ is required for FRC D (based on design using $R_{fr} = 6.5$ and $\Delta_{afr} = 1.75\%$), which is identical to the baseline value (so no change required).

## 4. CONCLUSIONS

This report documents the quantification of the functional recovery seismic performance factors for the DSMF system in accordance with the proposed Section A.8.3.6 procedures of the 2026 National Earthquake Hazards Reduction Program (NEHRP) Provisions. The functional recovery seismic performance factors include the functional recovery response modification coefficient, $R_{fr,}$, and functional recovery allowable story drift limit, $\Delta_{afr}$, and the $R_{\mu fr}$ for estimation of peak floor accelerations, which are summarized in Table 16 and Table 19, for the two design cases for fixed versus pinned connections in the damper frames, including the results from the analysis and the judgment-based limits of NEHRP 2026 Section A.8.3.6.

As shown in the previous sections, when damage occurred, safety-critical structural damage in the DSMF archetypes was primarily driven by steel moment connection and gravity component failures, although damper failure contributed more at a lower $\Delta_{afr}$. However, the analysis results showed that current ASCE/SEI 7 Chapter 12 Response modification factors and allowable story drift limits satisfied the prequalification procedure. Therefore, the recommended design parameters a controlled by the "judgment-based" upper limit of Section A.8.3.6 of the 2026 NEHRP Provisions.

Table 18. *Summary of functional recovery seismic performance factors for DSMFs (with fixed beam-to-column connections in damper frame).*

| | FRC A/B/C | | | FRC D | | |
|---|---|---|---|---|---|---|
| | $R_{fr}$ | $\Delta_{afr}$ | $R_{\mu fr}$ | $R_{fr}$ | $\Delta_{afr}$ | $R_{\mu fr}$ |
| Analysis results (case of fixed connection) | 6.0 | 1.25% | --† | 8.0 | 2.0% | --† |
| Strength-stiffness independent check | 6.0 | ~1.25%* | n/a | 8.0 | ~1.5%* | n/a |
| Judgment-based upper limit | 5.5 | 1.25% | n/a | 6.5 | 1.75% | n/a |
| **Recommendation – DSMF** | **5.5** | **1.25%** | **1.42** | **6.5** | **1.5%** | **1.55** |

*The strength-and-stiffness-independent check showed that $\Delta_{afr}$ of ~1.25% and ~1.5% for FRC A/B/C and FRC D, respectively, was required for the mid-rise performance group to meet the performance targets.

†*$R_{\mu fr}$ is only calculated for the recommended seismic performance factors.*

Table 19. *Summary of functional recovery seismic performance factors for DSMFs (with pinned beam-to-column connections in damper frame).*

| | FRC A/B/C | | | FRC D | | |
|---|---|---|---|---|---|---|
| | $R_{fr}$ | $\Delta_{afr}$ | $R_{\mu fr}$ | $R_{fr}$ | $\Delta_{afr}$ | $R_{\mu fr}$ |
| Analysis results (case of pinned connection) | 8.0 | 2.0% | --† | 8.0 | 2.0% | --† |
| Strength-stiffness independent check | 8.0 | 1.25%* | n/a | 8.0 | 1.5%* | n/a |
| Judgment-based upper limit | 5.5 | 1.25% | n/a | 6.5 | 1.75% | n/a |
| **Recommendation – DSMF** | **5.5** | **1.25%** | **1.42** | **6.5** | **1.5%** | **1.55** |

*The strength-and-stiffness-independent check showed that $\Delta_{afr}$ of 1.25% and 1.5% for FRC A/B/C and FRC D, respectively, was required for the mid-rise performance group to meet the performance targets.

†$R_{\mu fr}$ is only calculated for the recommended seismic performance factors.

## SUPPLEMENTARY MATERIAL

Two supplementary files are attached to this Prequalification Report that provide additional detailed information on the structural response and ATC 138 outcomes from individual archetype models and performance groups, as well as performance outcomes from the independent-strength-and-stiffness check discussed in the body of the report. The general description of the content contained in each file is provided below to assist with navigation and comprehension of detailed results.

- **Analysis Report Tables** *(“SupplementalData_AnalysisReportTables_DSMF_final(v1_3)_UPDATE_2.xls”*)
  - Contains detailed analysis outcomes for each archetype model assessed, including results for FRC A/B/C and FRC D.
  - “Summary” tab provides a summary of the controlling design values and other response metrics for each archetype
  - “All Runs” tab provides response and performance outcomes for all combinations of model runs for each archetype.
- **Archetype Performance Plots** *(“SupplementalData_ArchetypePerformancePlotsAppendix_DSMF_final(v1_3)_UPDATE.pdf”*)
  - Provides visualizations of analysis outcomes similar to the figures in the report, but for the independent-strength-and-stiffness check.
  - Provides visualizations of analysis outcomes similar to the figures in the report, but for individual archetype models.
  - Provide peak drift and peak floor acceleration response profiles for each archetype model.

## REFERENCES


Akcelyan, S., Lignos, D.G., Hikino, T., Nakashima, M. (2016). "Evaluation of Simplified and State-of-the-Art Analysis Procedures for Steel Buildings Equipped with Supplemental Damping Devices Based on E-Defense Full-Scale Shake Table Tests, *Journal of Structural Engineering, ASCE*, **142**(6): 04016024.

Akcelyan, S. (2017). "Seismic Retrofit of Existing Steel Tall Buildings with Supplemental Damping Devices, *PhD Dissertation*, McGill University, Montreal, Quebec, Canada.

Almeter, E., Wade, K.F., Haselton, C.B., Saxey, B. (2018). "Rapid Risk Assessment of Buckling Restrained Braced Frames, With Focus on Residual Drifts," *Proceedings of the 11th U.S. National Conference on Earthquake Engineering* (11NCEE), Los Angeles, CA.

ASCE. (2022). "Minimum Design Loads and Associated Criteria for Buildings and Other Structures," *ASCE/SEI 7-22*, American Society of Civil Engineers, Reston, VA.

ATC. (2021). "Seismic Performance Assessment of Buildings: Volume 8 – Methodology for Assessment of Functional Recovery Time, *ATC-138-3*, Preliminary report for FEMA P-58-8, Prepared by the Applied Technology Council for the Federal Emergency Management Agency, Washington, DC.

Blowes, K., Molina-Hutt, C., Zimmerman, R., Cook, D.T., Almeter, E., Haselton, C.B. (2025). "Limiting Safety-Critical Structural Damage in Recovery-Based Seismic Design Provisions," *Earthquake Spectra* (manuscript under review).

Bruneau, M., Mahin, S., Popov, E.P. (1987). "Ultimate Behavior of Butt-Welded Splices in Heavy Rolled Steel Sections," *EERC Report 87/10*, Univ. of Calif. at Berkeley.

Burda, J.J., Itani, A.M. (1999). "Studies of Seismic Behavior of Steel Base Plates." *Report No. CCEER 97-7*, Center for Civil Engineering Earthquake Research, Dept. of Civil Engineering, University of Nevada, Reno, Nevada.

Choi, J., Stojadinovic, B., Goel, S.C. (2000). "Parametric Tests on the Free Flange Connections," *Report No. SAC/BD-00/02*, SAC Joint Venture.

Cook, D., Wade, K., Haselton, C., Baker, J. W., & DeBock, D. J. (2018). A structural response prediction engine to support advanced seismic risk assessment. In *Eleventh US national conference on earthquake engineering, Los Angeles, CA*.

DeBock, D.J., Malatesta, A., Harris, J.R., Canney, N., Welch, D.P. (2023). "Taylor Damped Moment Frame System™: Report 1 – System Description," Prepared by Haselton Baker Risk Group for Taylor Devices Inc., North Tonawanda, NY.

DeBock, D., Manousakis, I.V., Deierlein, G.G., Zsarnóczay, A. (2024). "Updated Model and Criteria for Residual Drift," *FEMA P-58/BD-3.7.26*, Background documentation for the ATC-138/FEMA P-58 Project, Submitted to the Applied Technology Council, Prepared for the Federal Emergency Management Agency, Washington, DC.

Deierlein, G., Victorsson, V. (2008). “Fragility Curves for Components of Steel TDMF Systems,” *FEMA P-58/BD-3.8.3*, Background document for the FEMA P-58 project, Submitted to the Applied Technology Council and Prepared for the Federal Emergency Management Agency, Washington, DC.

Engelhardt, M.D., Venti, M.J. (2000). “Behavior and Design of Radius Cut Reduced Beam Section Connections,” *Report No. SAC/BD-00/17*, SAC Joint Venture.

Fahmy, M. (1999). “Seismic Behavior of Moment-Resisting Steel Column Bases” *PhD Dissertation*, Department of Civil and Environmental Engineering, University of Michigan, Ann Arbor, Michigan.

FEMA. (2009). “Quantification of Building Seismic Performance Factors,” *FEMA P695*, Prepared by the Applied Technology Council for the Federal Emergency Management Agency, Washington, DC.

FEMA. (2018a). “Seismic Performance Assessment of Buildings: Volume 1 - Methodology,” *FEMA P-58-1*, 2nd Edition, Prepared by the Applied Technology Council for the Federal Emergency Management Agency, Washington, DC.

FEMA. (2018b). “Seismic Performance Assessment of Buildings: Volume 2 – Implementation Guide,” *FEMA P-58-2*, 2nd Edition, Prepared by the Applied Technology Council for the Federal Emergency Management Agency, Washington, DC.

FEMA. (2018c). “Assessing Seismic Performance of Buildings with Configuration Irregularities,” *FEMA P-2012*, Prepared by the Applied Technology Council for the Federal Emergency Management Agency, Washington, DC.

Gilton, C., Chi., B., Uang, C.M. (2000). “Cyclic Testing of a Free Flange Moment Connection,” *Report No., SAC/BD-00/19*, SAC Joint Venture.

Gupta, A., Krawinkler, H. (1999) Seismic Demands for Performance Evaluation of Steel Moment Resisting Frame Structures, *Report No. 132*, John A. Blume Earthquake Engineering Center, Stanford University, Stanford, CA.

Hajjar, J.F., Lee, D., Dexter, R.J., Grauvilardell, J.E. (2005). “Synthesis of Design, Testing and Analysis on Steel Column Base Plate Connections in High-Seismic Zones,” *Structural Engineering Report No. St.-04-02*, Dept. of Civil Engineering, University of Minnesota.

Hartloper, A., Lignos, D.G. (2016). “Updates to the ASCE-41-13 Nonlinear Modeling Provisions for Performance-Based Seismic Assessment of New and Existing Steel Moment Resisting Frames,” *M.Eng. Thesis*, McGill University, Montreal, Canada.

Haselton, C.B., Deierlein, G.G. (2007). “Assessing seismic collapse safety of modern reinforced concrete frame buildings,” *Blume Center Technical Rep. No. 156,* Stanford University.

Haselton, C.B., Baker, J.W., Liel, A.B., Deierlein, G.G. (2011a). “Accounting for ground-motion spectral shape characteristics in structural collapse assessment through an adjustment for epsilon,” *Journal of Structural Engineering*, **137**(3): 332-344.

Haselton, C.B., Liel, A.B., Deierlein, G.G., Dean, B.S., Chou, J.H. (2011b). “Seismic Collapse Safety of Reinforced Concrete Buildings: I. Assessment of Ductile Moment Frames,” *Journal of Structural Engineering*, **137**(4): 481-491.

Haselton, C.B., Liel, A.B., Taylor-Lange, S.C., Deierlein, G.G. (2016). “Calibration of model to simulate response of reinforced concrete beam-columns to collapse,” *ACI Structural Journal*, **113**(6): 1141-1152.

Haselton Baker Risk Group (2025). Seismic Performance Prediction Program (SP3).

ICC-ES. (2018). “Acceptance Criteria for Qualification of Building Seismic Performance Factors of Alternative Seismic Force-Resisting Systems (ICC-ES Guidance Document to FEMA P695),” *AC494*, International Code Council Evaluation Service, Brea, CA.

ICC-ES. (2023). “Taylor Damped Moment Frame System (TDMF™),” *ICC-ES Evaluation Report ESR-4769.* International Code Council Evaluation Service, Brea, California.

Ibarra, L.F., Medina, R.A., Krawinkler, H. (2005). “Hysteretic models that incorporate strength and stiffness deterioration,” *Earthquake Engineering and Structural Dynamics*, **34**(12): 1489-1511.

Kim, T., Whittaker, A.S., Gilani, A.S.J., Bertero, V.V., Takhirov, S.M. (2002). “Cover-Plate and Flange-Plate Reinforced Steel Moment-Resisting Connections,” *Report No. SAC/BD-00/27*, SAC Joint Venture.

Krawinkler, H. (1978). Shear in beam-column joints in seismic design of steel frames, *Engineering Journal*, **15**(3): 82-91.

Liel, A.B., Deierlein, G.G. (2008). “Assessing the collapse risk of California’s existing reinforced concrete frame structures: Metrics for seismic safety decisions,” *Blume Center Technical Report No. 166*, Stanford University.

Liel, A.B., Haselton, C.B., Deierlein, G.G., Baker, J.W. (2009). “Incorporating Modeling Uncertainties in the Assessment of Seismic Collapse Risk of Buildings,” *Structural Safety*, **31**(2): 197-211.

Liel, A.B., Haselton, C.B., Deierlein, G.G. (2011). “Seismic Collapse Safety of Reinforced Concrete Buildings: II. Comparative Assessment of Non-Ductile and Ductile Moment Frames,” *Journal of Structural Engineering*, **137**(4): 492-502.

Lignos, D.G., Krawinkler, H. (2011). “Deterioration Modeling of Steel Components in Support of Collapse Prediction of Steel Moment Frames under Earthquake Loading,” *Journal of Structural Engineering*, **137**(11): 1291-1302.

Lignos, D.G., Hartloper, A.R., Elkady, A., Deierlein, G.G., Hamburger, R. (2019). "Proposed Updates to ASCE 41 Nonlinear Modeling Parameters for Wide-Flange Steel Columns in Support of Performance-Based Seismic Engineering," *Journal of Structural Engineering*, **145**(9): 04019083.

Liu, J., Astaneh-Asl, A. (2000). "Cyclic testing of simple connections including effects of slab," *Journal of Structural Engineering*, **126**(1): 32-39.

Miranda, E. (1999). "Approximate seismic lateral deformation demands in multistory buildings," *Journal of Structural Engineering*, **125**(4): 417-425.

Miranda, E., Reyes, C.J. (2002). "Approximate lateral drift demands in multistory buildings with nonuniform stiffness," *Journal of Structural Engineering*, **128**(7): 840-849.

McKenna, F., Scott, M.H., Fenves, G.L. (2010). "Nonlinear Finite-Element Analysis Software Architecture using Object Composition," *Journal of Computing in Civil Engineering*, **24**(1): 95-107.

NIST. (2010). "Evaluation of the FEMA P-695 Methodology for Quantification of Building Seismic Performance Factors," *NIST GCR 10-917-08*, National Institute of Standards and Technology, Gaithersburg, MD.

NIST. (2017). "Guidelines for Nonlinear Structural Analysis and Design of Buildings: Part IIa – Steel Moment Frames," *NIST GCR 17-917-46v2*, Prepared by the Applied Technology Council for the National Institute of Standards and Technology (NIST), Gaithersburg, MD.

Nuttayasakul, N. (2001). "Finite element fracture mechanics study of partial penetration welded splices," *Engineer Degree Thesis*, Stanford University.

Ricles, J.M., Mao, C., Lu, L.-W., Fisher, W. (2000). "Development and Evaluation of Improved Details for Ductile Welded Unreinforced Flange Connections," *Report No. SAC/BD-00/24*, SAC Joint Venture.

Ricles, J.M., Zhang, X., Lu, L., Fisher, J. (2004). "Development of Seismic Guidelines for Deep-Column Steel Moment Connections," *ATLSS Report No. 04-13*.

Skiadopoulos, A., Elkady, A., Lignos, D.G. (2021). "Proposed Panel Zone Model for Seismic Design of Steel Moment-Resisting Frames," *Journal of Structural Engineering*, **147**(4): 04021006.

Taylor Devices. (2023). "Personal communication regarding damper damage states and fragility assumptions," May 3, 2023, Meeting with Nathan Canney from Taylor Devices, Inc.

Vamvatsikos, D., Cornell, C.A. (2002). "Incremental Dynamic Analysis," *Earthquake Engineering and Structural Dynamics*, **31**(3): 491-514.

Venti, M.J., Engelhardt, M.D. (2000). “Test of a Free Flange Connection with a Composite Floor Slab,” *Report No. SAC/BD-00/18*, SAC Joint Venture

Vouvakis Manousakis I., Zsarnoczay A., Konstantinidis D., (2024), “Robust Residual Drift Estimation for Seismic Performance Assessment based on High-Fidelity Response Simulation of Steel Frames,” (manuscript in preparation).

Welch, D.P., DeBock, D.J., Harris, J.R., Malatesta, A., Canney, N., Burton, H., Guan, X., Sabol, T. (2023a). “Taylor Damped Moment Frame System™: Report 2 – Archetype Designs for Collapse Analysis,” Prepared by Haselton Baker Risk Group for Taylor Devices Inc., North Tonawanda, NY.

Welch, D.P., DeBock, D.J. (2023a). “Taylor Damped Moment Frame System™: Report 3 – Nonlinear Modeling of Index Archetypes,” Prepared by Haselton Baker Risk Group for Taylor Devices Inc., North Tonawanda, NY.

Welch, D.P., DeBock, D.J., Harris, J.R. (2023b). “Taylor Damped Moment Frame System™: Report 4 – Collapse Performance of Index Archetypes,” Prepared by Haselton Baker Risk Group for Taylor Devices Inc., North Tonawanda, NY.

Welch, D.P., DeBock, D.J., Haselton, C.B. (2023c). “FEMA P-58 Fragility Development for the Taylor Damped Moment Frame™ (TDMF™),” Prepared by Haselton Baker Risk Group for Taylor Devices Inc., North Tonawanda, NY.